

Article

# Molecular and Supramolecular Structures of Cd(II) Complexes with Hydralazine-Based Ligands; A New Example for Cyclization of Hydrazonophthalazine to Triazolophthalazine

Saied M. Soliman <sup>1,\*</sup>, Raghdaa A. Massoud <sup>1</sup>, Hessa H. Al-Rasheed <sup>2,\*</sup> and Ayman El-Faham <sup>1,2</sup>

<sup>1</sup> Department of Chemistry, Faculty of Science, Alexandria University, P.O. Box 426, Ibrahimia, Alexandria 21321, Egypt; raghdaamassoud@yahoo.com (R.A.M.); aelfaham@ksu.edu.sa (A.E.-F.)

<sup>2</sup> Department of Chemistry, College of Science, King Saud University, P.O. Box 2455, Riyadh 11451, Saudi Arabia

\* Correspondence: saeed.soliman@alexu.edu.eg (S.M.S.); halbahli@ksu.edu.sa (H.H.A.-R.); Tel.: +20-1111361059 (S.M.S.); +966-114673195 (H.H.A.-R.)

**Abstract:** Molecular and supramolecular structures of two polymeric and one trinuclear Cd(II) complex with hydralazine-type ligands were presented. Self-assembly of *E*-1-(2-(thiophen-2-ylmethylene)hydrazinyl)phthalazine (HL) and CdCl<sub>2</sub> gave the 1D coordination polymer [Cd(H<sub>2</sub>L)Cl<sub>3</sub>]<sub>n</sub>·H<sub>2</sub>O, **1**, in which the Cd(II) ion is hexa-coordinated with one cationic monodentate ligand (H<sub>2</sub>L<sup>+</sup>) and five chloride ions, two of them acting as connectors between Cd(II) centers, leading to the formation of a 1D coordination polymer along the *a*-direction. Using DFT calculations, the cationic ligand (H<sub>2</sub>L<sup>+</sup>) could be described as a protonated HL with an extra proton at the hydrazone moiety. Repeating the same reaction by heating under reflux conditions in the presence of 1 mL saturated aqueous KSCN solution, the ligand HL underwent cyclization to the corresponding [1,2,4]triazolo[3,4-*a*]phthalazine-3(2H)-thione (TPT) followed by the formation of [Cd(TPT)(SCN)<sub>2</sub>]<sub>n</sub>·H<sub>2</sub>O, **2**, a 1D coordination polymer. In this complex, the Cd(II) is coordinated with one *NS*-donor TPT bidentate chelate and two bridged  $\mu(1,3)$ -thiocyanate ions connecting the Cd(II) centers forming the 1D polymer array along the *b*-direction. Heating *E*-2-(1-(2-(phthalazin-1-yl)hydrazono)ethyl)phenol HL<sup>OH</sup> with CdCl<sub>2</sub> under reflux condition gave the trinuclear complex [Cd<sub>3</sub>(Hydralazine)<sub>2</sub>(H<sub>2</sub>O)<sub>2</sub>Cl<sub>6</sub>], **3**, indicating the hydrolysis of the hydrazonophthalazine ligand HL<sup>OH</sup> during the course of the reaction. Due to symmetry considerations, there are only two different Cd(II) centers having CdN<sub>2</sub>Cl<sub>3</sub>O and CdN<sub>2</sub>Cl<sub>4</sub> coordination environments. Hirshfeld topology analysis was used to analyze the solid-state supramolecular structure of the studied complexes.

**Keywords:** Cd(II); hydrazonophthalazine; triazolophthalazine; Hirshfeld; tautomerism; cationic ligand



**Citation:** Soliman, S.M.; Massoud, R.A.; Al-Rasheed, H.H.; El-Faham, A. Molecular and Supramolecular Structures of Cd(II) Complexes with Hydralazine-Based Ligands; A New Example for Cyclization of Hydrazonophthalazine to Triazolophthalazine. *Crystals* **2021**, *11*, 823. <https://doi.org/10.3390/cryst11070823>

Academic Editor: Alexander Pöthig

Received: 2 July 2021

Accepted: 13 July 2021

Published: 15 July 2021

**Publisher's Note:** MDPI stays neutral with regard to jurisdictional claims in published maps and institutional affiliations.



**Copyright:** © 2021 by the authors. Licensee MDPI, Basel, Switzerland. This article is an open access article distributed under the terms and conditions of the Creative Commons Attribution (CC BY) license (<https://creativecommons.org/licenses/by/4.0/>).

## 1. Introduction

Phthalazine derivatives have been the subject of substantial studies in recent years due to their interesting medicinal applications as efficient anti-inflammatory [1,2], antimicrobial [3–10], anticonvulsant [11], and anticancer agents [12–14]. On the other hand, hydralazine (1-hydrazinophthalazine) is a well-known nitrogen heterocycle which is a clinically accepted drug in the chemotherapy of hypertension [15]. Furthermore, derivatives of hydralazine have widespread use in the treatment of many diseases, such as tuberculosis and mental disorders [16]. Additionally, 1-chlorophthalazine derivatives are considered as significant components in the design of biologically such active molecules as tetrazole, triazole, imidazole, pyrimidine, piperazine, and triazine [17–21].

Schiff bases derived from hydralazine also have considerable importance in the discipline of coordination chemistry as they are regarded as strong electron donor ligands able to coordinate metal ion through their *N*-chelating sites. The denticity of the ligand could

be improved by adding substituents having donor atoms, such as nitrogen, oxygen, or sulphur [15]. In this regard, binuclear metal (II) complexes with phthalazine type ligands were found to have interesting magnetic interactions and were also used as good examples of metalloenzymes and in catalysis applications [22]. Moreover, Schiff bases derived from hydralazine could act as a good receptor for the transition metals, causing remarkable color change, and hence could be used as chemosensors [23,24].

Cadmium is an exceedingly poisonous heavy metal [25–28]. On the other hand, it was found to serve as a catalytic center in the carbonic anhydrase [29]. In addition, Cd(II) compounds have potential applications in optical areas [30–33]. Cd(II) complexes with nitrogen-containing ligands have also been successfully used in ligand exchange chromatography [34–36]. The coordination compounds of Cd(II) have received increased attention due to their interesting structures and versatile applications in nanotechnologies [37–40]. Moreover, they have interesting DNA binding abilities [41–43], antibacterial activities [44,45], antitumor properties [46,47], and are known catalysts for organic transformations [48–53].

In literature, Cd(II) has very flexible coordination sphere with coordination numbers ranging from four to eight. Moreover, phthalazine ligands have different coordination modes [54,55]. Complex formation between phthalazine (Phtz) and Cd(II) ion in the presence of pseudohalides ( $\text{N}_3^-$ ,  $\text{N}(\text{NC})_2^-$ , and  $\text{NCS}^-$ ) afforded the  $[\text{Cd}(\text{Phtz})(\text{MeOH})(\text{N}_3)_2]_n$  and  $[\text{Cd}(\text{Phtz})_2(\text{dca})_2]_n$  one dimensional polymers and the discrete dinuclear  $[\text{Cd}(\text{SCN})_2(\text{Ptz})_2(\text{H}_2\text{O})]_2$ , respectively. Here, Phtz is acting as a terminal monodentate ligand via one of its nitrogen atoms in the  $[\text{Cd}(\text{Phtz})_2(\text{dca})_2]_n$  and  $[\text{Cd}(\text{SCN})_2(\text{Ptz})_2(\text{H}_2\text{O})]_2$  complexes. On the other hand, it acts as a *NN*-connector between the Cd(II) centers in the azido complex [56]. In our previous work, Schiff bases derived from hydralazine were found to be powerful mononegative [15] or neutral [57] tridentate *N*-chelators. Moreover, the same ligands underwent Cu(II)-promoted oxidation with cyclization to afford the corresponding triazolophthalazine [58]. In light of the interesting coordination chemistry of Cd(II) and the interesting chelating power of hydrazonophthalazine ligands, which are considered as important topics in the field of crystal engineering [59], the aim of the present work is to shed the light on the molecular and supramolecular structure diversities of novel Cd(II) complexes with the two phthalazine-type ligands (HL and HL<sup>OH</sup>) shown in Figure 1.

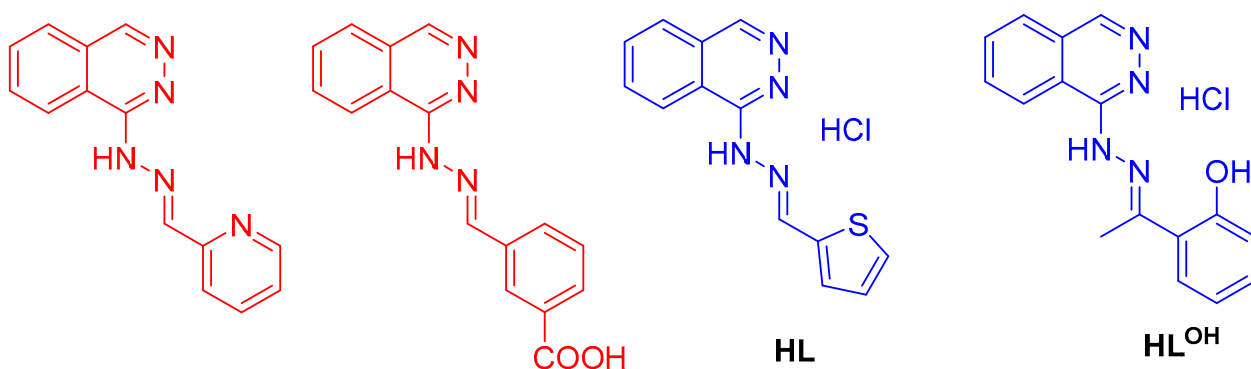


**Figure 1.** Structure of the studied hydralazine-based ligands; red color: previously reported ligand [15,57]; blue color: new ligands.

## 2. Materials and Methods

### 2.1. Materials and Physical Measurements

Chemicals were purchased from Sigma-Aldrich Company (Chemie GmbH, Taufkirchen, Germany). CHN analyses were performed using Perkin Elmer 2400 Elemental Analyzer (PerkinElmer, Inc.940 Winter Street, Waltham, MA, USA). Cadmium content was determined using Shimadzu atomic absorption spectrophotometer (AA-7000 series, Shimadzu,

Ltd., Tokyo, Japan). An Alpha Bruker spectrophotometer (Billerica, MA, USA) was used to measure the FTIR spectra in KBr pellets.

## 2.2. Synthesis

### 2.2.1. Synthesis of HL and HL<sup>OH</sup>

The hydrazonophthalazine ligands (HL and HL<sup>OH</sup>) were prepared using the method recently described by our group [15,58]. A mixture of hydralazine-HCl (10 mmol) and sodium acetate (10 mmol) in 50 mL of ethanol was stirred at room temperature for 2 min. Then, a solution of aldehyde or ketone (10 mmol) in 10 mL ethanol was added dropwise. The reaction mixture was refluxed for 4 h and then left to cool at room temperature. The yellow precipitate was filtered, and the pure product (HL and HL<sup>OH</sup>) was obtained by recrystallization from ethanol as yellow crystals.

(*E*)-1-(2-(thiophen-2-ylmethylene)hydrazinyl)phthalazine hydrochloride; HL Yield; C<sub>13</sub>H<sub>11</sub>ClN<sub>4</sub>S (HL) 89%, mp 241–3 °C. Anal. Calc. C, 53.70; H, 3.81; N, 19.27; S, 11.03. Found: C, 53.91; H, 3.88; N, 19.43; S, 11.27. <sup>1</sup>H NMR (DMSO-*d*<sub>6</sub>) δ (HL): 7.23(t, 1H, *J* = 3.6 Mz), 7.78 (d, 1H, *J* = 3.2 Hz), 7.88((d, 1H, *J* = 5.2 Hz), 8.13–8.21 (m, 4H), 8.90 (d, 1H, *J* = 8.0 Hz), 8.99 (s, 1H), 9.10 (s, 1H) ppm; <sup>13</sup>C NMR (DMSO-*d*<sub>6</sub>) δ (HL): 119.9, 125.4, 128.3, 128.8, 128.9, 132.5, 134.2, 136.4, 137.8, 144.9, 148.2, 148.3 ppm (Supplementary Figures S1 and S2).

(*E*)-2-(1-(2-(Phthalazin-1-yl)hydrazono)ethyl)phenol hydrochloride; HL<sup>OH</sup> Yield; C<sub>16</sub>H<sub>15</sub>ClN<sub>4</sub>O (HL<sup>OH</sup>) 91%, mp 254–6 °C. Anal. Calc. C, 61.05; H, 4.80; N, 17.80. Found: C, 61.23; H, 4.94; N, 17.99. <sup>1</sup>H NMR (DMSO-*d*<sub>6</sub>) δ (HL): 6.88(t, 1H, *J* = 8.0 Mz), 6.94 (d, 1H, *J* = 8.0 Hz), 7.29((t, 1H, *J* = 8.0 Hz), 7.71 (d, 1H, *J* = 8.0 Hz), 7.98–8.11 (m, 3H), 8.76 (brd, 1H), 8.87 (brs, 1H) ppm; <sup>13</sup>C NMR (DMSO-*d*<sub>6</sub>) δ (HL<sup>OH</sup>): 17.1, 113.7, 116.8, 118.7, 121.8, 124.4, 125.1, 126.9, 127.3, 127.7, 129.5, 131.6, 133.2, 134.5, 135.3, 157.8 ppm (Supplementary Figures S3 and S4).

### 2.2.2. Synthesis of [Cd(H<sub>2</sub>L)Cl<sub>3</sub>]<sub>n</sub>·H<sub>2</sub>O; 1

A 10 mL methanolic solution of HL (0.029 g, 0.1 mmol) was mixed with 5 mL aqueous solution of CdCl<sub>2</sub> (0.018 g, 0.1 mmol). The solution mixture was left for a week for slow evaporation at room temperature. Colorless crystals of **1** were obtained, filtered, and were found suitable for X-ray single crystal structure measurements.

C<sub>13</sub>H<sub>13</sub>CdCl<sub>3</sub>N<sub>4</sub>OS (**1**) (84% yield). Anal. Calc. C, 31.73; H, 2.66; N, 11.39; Cd, 22.84%. Found: C, 31.61; H, 2.59; N, 11.27; Cd, 22.70 %. IR (KBr, cm<sup>-1</sup>): 3445, 3399, 3078, 2125, 1624, 1589, 1577 (Supplementary Figure S5).

### 2.2.3. Synthesis of [Cd(TPT)(SCN)<sub>2</sub>]<sub>n</sub>·H<sub>2</sub>O; 2

A 10 mL methanolic solution of HL (0.029 g, 0.1 mmol) was mixed with a 5 mL aqueous solution of CdCl<sub>2</sub> (0.018 g, 0.1 mmol) then 1 mL of a saturated aqueous solution of KSCN was added. The mixture was heated under reflux for 2 h followed by filtration. The clear solution was left for three days for slow evaporation; yellow crystals of **2** were isolated from the solution by filtration.

C<sub>11</sub>H<sub>8</sub>CdN<sub>6</sub>OS<sub>3</sub> (**2**) (77% yield). Anal. Calc. C, 29.44; H, 1.80; N, 18.72; Cd, 25.05 %. Found: C, 29.30; H, 1.74; N, 18.60; Cd, 24.89 %. IR (KBr, cm<sup>-1</sup>): 3456, 3066, 2922, 2065, 1613, 1589, 1515 (Supplementary Figure S6).

### 2.2.4. Synthesis of [Cd<sub>3</sub>(Hydralazine)<sub>2</sub>(H<sub>2</sub>O)<sub>2</sub>Cl<sub>6</sub>]; 3

A 10 mL methanolic solution of HL<sup>OH</sup> (0.032 g, 0.1 mmol) was mixed with 5 mL aqueous solution of CdCl<sub>2</sub> (0.018 g, 0.1 mmol). The mixture was heated under reflux for 2 h followed by filtration. The clear solution was left for three days for slow evaporation; colorless crystals of **3** were isolated from the solution by filtration.

C<sub>16</sub>H<sub>20</sub>N<sub>8</sub>Cl<sub>6</sub>Cd<sub>3</sub>O<sub>2</sub> (**2**) (77% yield). Anal. Calc. C, 21.20; H, 2.22; N, 12.36; Cd, 37.21%. Found: C, 21.09; H, 2.17; N, 12.25; Cd, 37.04 %. IR (KBr, cm<sup>-1</sup>): 3626, 3295, 3059, 3024, 1619, 1593, 1518 (Supplementary Figure S7).

### 2.3. Methods and Calculations

Geometry optimizations of the possible tautomers of the ligand HL and its protonated form (Figure 2) were performed using the MPW1PW91/TZVP method with the aid of Gaussian 09 software [60]. All frequencies have positive values, which indicated real energy minimum structures. The results of the calculated thermodynamic parameters were used to predict the most stable tautomer and to calculate the proton affinity of the ligand HL.

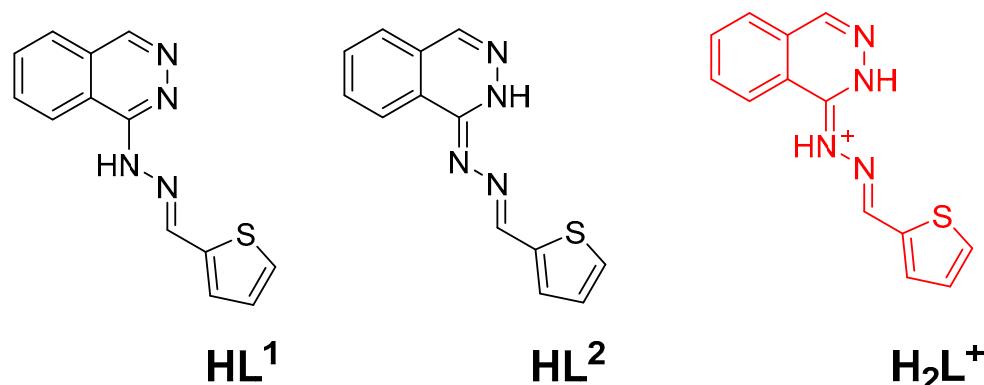


**Figure 2.** The possible tautomers of the ligand HL and its protonated form.

### 2.4. Crystal Structure Determination

The crystal structures of the studied Cd(II) complexes were determined by using a Bruker D8 Quest diffractometer employing SHELXTL and SADABS programs [61–63]. All crystal data and refinement details are listed in Table 1. Hirshfeld calculations were performed using Crystal Explorer 17.5 program [64–69].

**Table 1.** Crystal data and refinement details of the studied complexes.

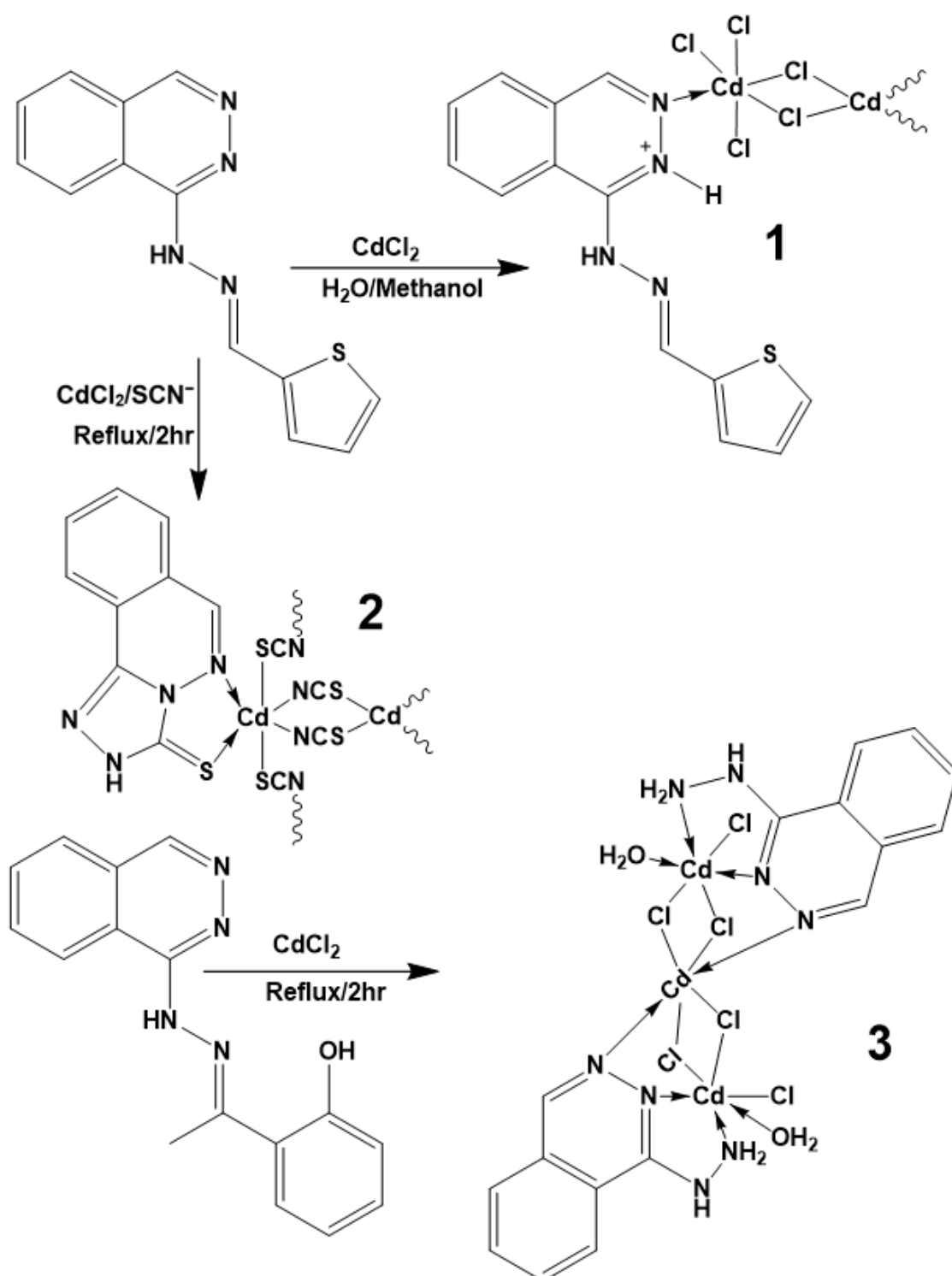
Compound	1	2	3
Empirical formula	C <sub>13</sub> H <sub>13</sub> CdCl <sub>3</sub> N <sub>4</sub> OS	C <sub>11</sub> H <sub>8</sub> CdN <sub>6</sub> OS <sub>3</sub>	C <sub>8</sub> H <sub>10</sub> N <sub>4</sub> Cl <sub>3</sub> Cd <sub>1.5</sub> O
Formula weight (g/mol)	492.08	448.81	453.15
Temperature (K)	293(2)	115(2)	293.15
λ (Å)	0.71073	0.71073	0.71073
Crystal system	Triclinic	Triclinic	Triclinic
Space group	P-1	P-1	P-1
Unit cell dimensions			
a (Å)	a = 7.277(3)	a = 7.0680(6)	6.972(3)
b (Å)	b = 11.451(5)	b = 10.0072(9)	10.706(4)
c (Å)	c = 12.042(5)	c = 10.9572(9)	11.887(5)
α (°)	α = 110.994(9)	α = 83.385(5)	67.966(10)
β (°)	β = 99.076(9)	β = 84.500(5)	77.907(11)
γ (°)	γ = 107.083(8)	γ = 80.595(5)	81.146(12)
Volume (Å <sup>3</sup> )	855.7(6)	757.16(11)	801.4(6)
Z	2	2	2
Density (calculated, g/cm <sup>3</sup> )	1.910	1.969	1.878
Absorption coefficient (mm <sup>-1</sup> )	1.873	1.864	2.499
F(000)	484	440	434
Crystal size, mm <sup>3</sup>	0.15 × 0.17 × 0.27	0.143 × 0.176 × 0.299	0.3 × 0.23 × 0.12
θ range	2.12 to 25.00°	2.65 to 25.00°	5.996 to 49.992°

Table 1. Cont.

Compound	1	2	3
Index ranges	$-8 \leq h \leq 8,$ $-13 \leq k \leq 13,$ $-14 \leq l \leq 14$	$-8 \leq h \leq 8,$ $-11 \leq k \leq 11,$ $-13 \leq l \leq 13$	$-8 \leq h \leq 8,$ $-12 \leq k \leq 12,$ $-14 \leq l \leq 13$
Reflections collected	31488	10710	7897
Independent reflections	3023 [R(int) = 0.0360]	2660 [R(int) = 0.0497]	2805 [R <sub>int</sub> = 0.0523]
Completeness to theta	99.90%	99.60%	99.4%
Refinement method	Full-matrix least-squares on F <sup>2</sup>	Full-matrix least-squares on F <sup>2</sup>	Full-matrix least-squares on F <sup>2</sup>
Data/restraints/parameters	3023/3/224	2660/0/207	2805/0/162
Goodness-of-fit on F <sup>2</sup>	1.061	1.077	1.092
Final R indices [I > 2sigma(I)]	R1 = 0.0295, wR2 = 0.0712	R1 = 0.0364, wR2 = 0.1003	R <sub>1</sub> = 0.0427, wR <sub>2</sub> = 0.1094
R indices (all data)	R1 = 0.0366, wR2 = 0.0751	R1 = 0.0409, wR2 = 0.1054	R <sub>1</sub> = 0.0503, wR <sub>2</sub> = 0.1167
Largest diff. peak and hole	0.916/−0.661 Å <sup>−3</sup>	1.729/−1.325 Å <sup>−3</sup>	0.94/−1.25 Å <sup>−3</sup>
CCDC No.	2093653	2093654	2093655

### 3. Results

Hydrazonophthalazine ligands are powerful nitrogen chelators due to the availability of different coordinating sites, including the phthalazine and hydrazone nitrogen atoms. This class of ligands can coordinate to the metal ion in different ways depending on the nature of metal ion and reaction conditions [15,57,58]. In the case of easily oxidized metal ions such as Co(II), which can undergo aerobic oxidation in the presence of a strong ligand field, the ligand can lose the labile NH proton and work as a negatively charged *N*-chelator [15]. In another instance, the reaction with metal ions with stable oxidation states such as holmium(III), the ligand works as a neutral *N*-chelator [57]. On the other hand, hydrazonophthalazine underwent oxidative cyclization to the corresponding triazolophthalazines in presence of metal ions having well known catalytic activity such as Cu(II) [58]. In the current work, we presented the reactions of two new hydrazonophthalazine ligands with cadmium chloride as shown in Scheme 1. The molecular and supramolecular structures of the resulting one-dimensional coordination polymers **1** and **2** and the trinuclear complex **3** were elucidated with the aid of single crystal X-ray diffraction combined with Hirshfeld calculations.



Scheme 1. Synthesis of complexes 1–3.

#### 4. Discussion

##### 4.1. X-ray Crystal Structure Description

##### 4.1.1. $[\text{Cd}(\text{H}_2\text{L})\text{Cl}_3]_n \cdot \text{H}_2\text{O}$ Complex; (1)

The  $[\text{Cd}(\text{H}_2\text{L})\text{Cl}_3]_n \cdot \text{H}_2\text{O}$  complex (1) crystallized in the triclinic crystal system and the primitive P-1 space group. The hydrazonophthalazine ligand was found protonated either at the hydrazono or phthalazine N-atoms during the course of preparation while

the other *N*-site of the phthalazine moiety was found coordinated with the Cd(II) ion with a relatively long Cd1-N2 bond (2.773(4) Å). The asymmetric unit of **1** comprised one protonated organic H<sub>2</sub>L<sup>+</sup> molecule as a cationic monodentate ligand and three coordinated chloride anions as an anionic ligand (Figure 3; left part).

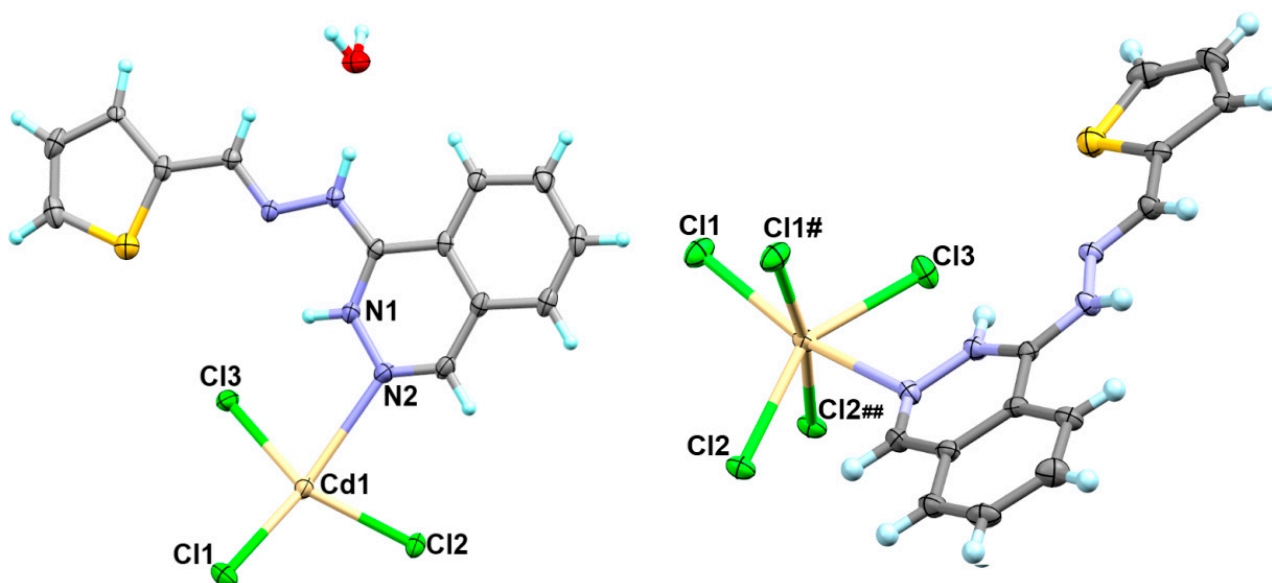


Figure 3. Asymmetric unit (left) and coordination sphere (right) with atom numbering for **1**.

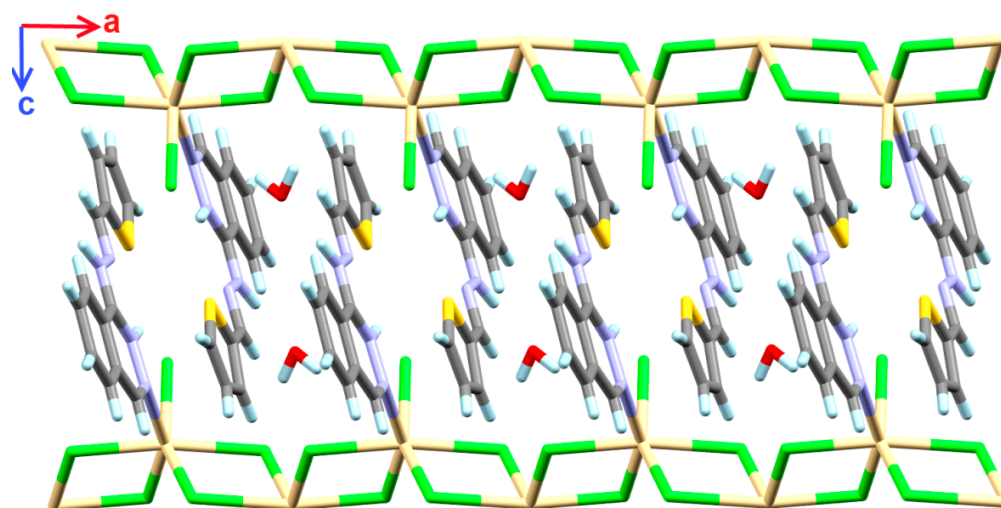
In this complex, the central metal ion could be described as hexa-coordinated with one H<sub>2</sub>L<sup>+</sup>, one terminal chloride (Cl3) and four bridging chloride ions (Cl1 and Cl2). Each two symmetrically related bridged chloride ions are related to one another by an inversion center; hence the asymmetric unit comprised only three chloride ions. The complete coordination sphere of this complex is shown in Figure 3 (right part) while the list of bond distances and angles are given in Table 2. It is clear that the terminal Cd1-Cl3 bond is the shortest (2.497(1) Å) among the other Cd-Cl interactions. The other chloride anions (Cl1 and Cl2) connecting the Cd1 centers with inequivalent Cd-Cl distances for each. The symmetrically related chloride ions are located *cis* to each other and found coordinated with the Cd1 with one short and one long Cd-Cl bonds. The Cd1-Cl1 and Cd1-Cl1# distances are 2.563(1) and 2.677(1) Å, respectively while the corresponding Cd1-Cl2 and Cd1-Cl2## distances are 2.517 and 2.858 Å, respectively. The coordination geometry around Cd1 could be described as a highly distorted octahedral with continuous shape measurements of 4.35 and 7.79 compared to the perfect octahedron and trigonal prism, respectively [69–72].

Table 2. Bond distances (Å) and angles (°) for **1**.

Atoms	Distance	Atoms	Distance
Cd1-N2	2.773(4)	Cd1-Cl1	2.563(1)
Cd1-Cl3	2.497(1)	Cd1-Cl1 #	2.677(1)
Cd1-Cl2	2.517(1)	Cd1-Cl2 ##	2.858(1)
Atoms	Angle	Atoms	Angle
Cl3-Cd1-Cl2	147.56(4)	Cl2-Cd1-Cl2 ##	79.43(4)
Cl3-Cd1-Cl1	103.19(5)	Cl1-Cd1-Cl2 ##	89.46(4)
Cl2-Cd1-Cl1	106.08(5)	N2-Cd1-Cl1	157.21(8)
Cl3-Cd1-Cl1 #	99.06(4)	N2-Cd1-Cl1 #	74.32(8)
Cl2-Cd1-Cl1 #	98.03(4)	N2-Cd1-Cl2	80.70(8)
Cl1-Cd1-Cl1 #	83.12(4)	N2-Cd1-Cl2 ##	113.29(8)
Cl3-Cd1-Cl2 ##	87.22(4)	N2-Cd1-Cl3	77.68(8)

# 1-X,1-Y,-Z; ## 2-X,1-Y,-Z

As a result of the *cis*-configuration of each two symmetrically related bridged chloride ions, the Cd1-Cl1-Cd1<sup>#</sup>-Cl1<sup>#</sup> and Cd1-Cl2-Cd1<sup>#</sup>-Cl2<sup>#</sup> formed four membered rings in the 1D polymer array, as shown in Figure 4. The four membered rings have the shape of a parallelogram with equidistant parallel sides. The Cd1-Cl1-Cd1<sup>#</sup> and Cd1-Cl2-Cd1<sup>#</sup> angles are found to be ~96.88 and 100.57°, respectively. As shown in Figure 4, the 1D coordination polymer extended along the crystallographic *a*-direction via the bridged Cd-Cl coordination interactions while the coordinated organic ligand was found in between two of these chains and the crystal water as well.



**Figure 4.** The 1D coordination polymer extended along the crystallographic *a*-direction via the Cd-Cl1/Cl2 interactions.

In addition to these coordination interactions, these chains are further connected by hydrogen bonding interactions mainly through the crystallized water molecule. All chloride ions are also shared in the hydrogen bonding interactions with the neighboring hydrogen bond donor groups. A list of the most important hydrogen bonds is given in Table 3 and depicted in Figure 5 (upper part). The terminal chloride ion (Cl3) shared in one intramolecular N1-H3A...Cl3 and another intermolecular O1-H1A...Cl3 hydrogen bond with the crystal water. In addition, the other chloride ions (Cl1 and Cl2) formed strong and weak hydrogen bonds with the crystal water (O1-H1B) and the thiophene moiety (C11-H11), respectively. The lower part of Figure 5 shows the two-dimensional supramolecular structure of **1** formed through the Cd-Cl coordination interactions and the hydrogen bonding interactions as well.

**Table 3.** The hydrogen bond parameters in **1**.

D-H...A	D-H (Å)	H...A (Å)	D...A (Å)	D-H...A(°)	Symm. Code
O1-H1A...Cl3	0.83(8)	2.62(9)	3.289(5)	140(7)	1-x,1-y,1-z
O1-H1B...Cl2	0.84(4)	2.39(4)	3.210(4)	167(6)	x,y,-1+z
N3-H5A...O1	0.91(5)	1.87(5)	2.762(6)	167(4)	x,y,z
C6-H6...O1	0.93	2.51	3.372(6)	154	x,y,z
C11-H11...Cl1	0.93	2.76	3.563(4)	145	x,y,-1+z

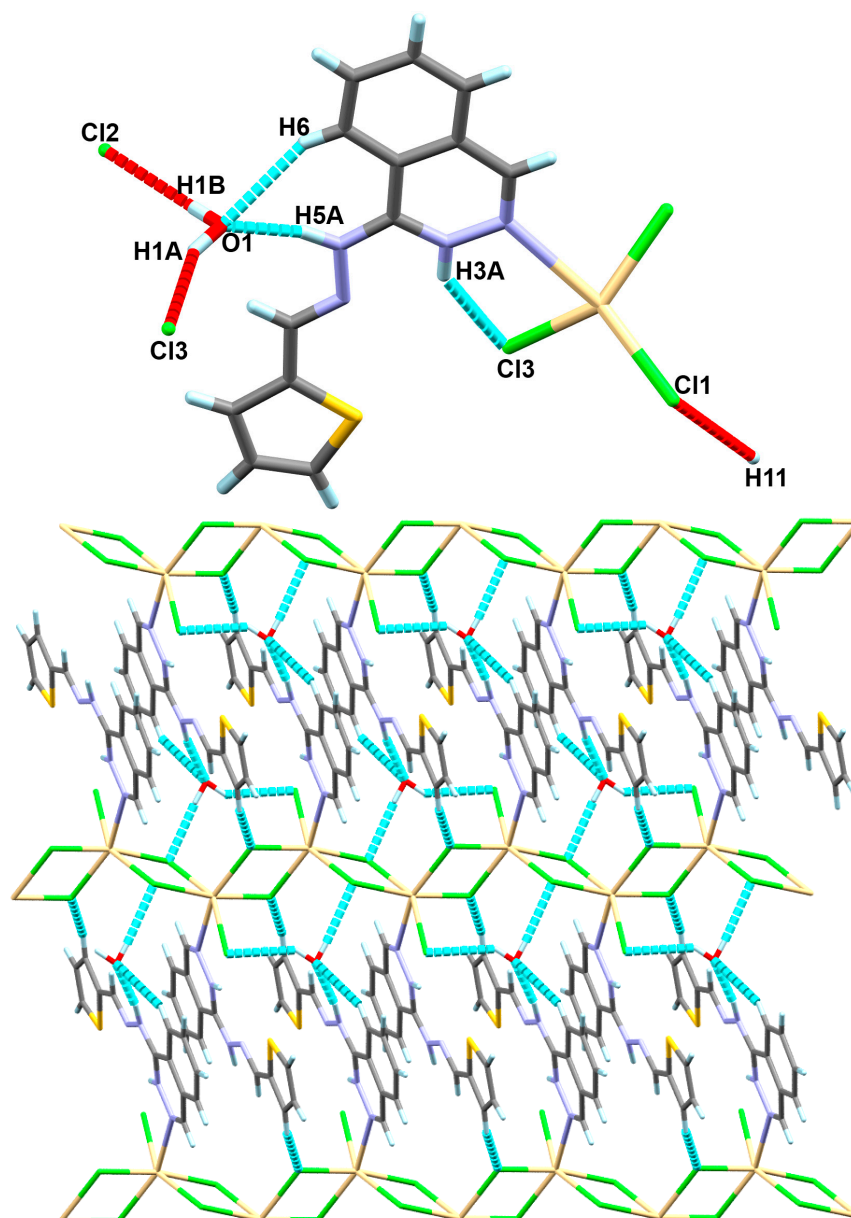


**Figure 5.** The hydrogen bond contacts (**upper**) and the hydrogen bonding network (**lower**) connecting the Cd-Cl chains via the O...H hydrogen bonds.

#### 4.1.2. $[\text{Cd}(\text{TPT})(\text{SCN})_2]_n \cdot \text{H}_2\text{O}$ Complex; (2)

The crystal structure of  $[\text{Cd}(\text{TPT})(\text{SCN})_2]_n \cdot \text{H}_2\text{O}$ , **2**, is shown in Figure 6. Interestingly, the reaction of hydrazonophthalazine (HL) with  $\text{CdCl}_2$  in the presence of thiocyanate under reflux condition provided the corresponding triazolophthalazine-thione (TPT; Scheme 1). This indicated that the thiocyanate assisted the cyclization-sulphurization process to the TPT ligand which underwent in situ complexation with Cd(II) to furnish the final product **2**. In this complex, the asymmetric unit comprised one TPT ligand as *NS*-bidentate chelator, and two bridged thiocyanate ions connecting the Cd1 centers in the  $\mu(1,3)$  coordination mode. Moreover, the Cd(II) is hexa-coordinated as found in complex **1**. The coordination sphere around Cd(II) comprised one TPT bidentate chelator (Cd1-N4: 2.480(3) Å, Cd1-S2: 2.636(1) Å and the bite angle is 77.51(8)°), and four  $\text{SCN}^-$  ions where each two symmetrically related thiocyanate groups are in *cis*-configuration. The distances between Cd1 and the thiocyanate *N*-atoms are 2.256(4) Å (Cd1-N2) and 2.338(4) Å (Cd1-N6) while the Cd-S(*thiocyanate*) distances are 2.741(1) Å and 2.749(1) Å for Cd1-S3 and Cd1-S1, respectively

(Table 4). The N-Cd-S angles of the two symmetrically related thiocyanate groups are  $88.41(9)^\circ$  and  $95.93(9)^\circ$  for N6-Cd1-S1 and N2-Cd1-S3, respectively while the angle between the trans S1-Cd1-S3 bond is  $166.02(3)^\circ$ . The continuous shape measurements for the coordination environment of Cd(II) in **2** are 0.866 and 15.829 compared to the perfect octahedron and trigonal prism, respectively. Hence, the CdN<sub>3</sub>S<sub>3</sub> coordination geometry could be described as a distorted octahedron.

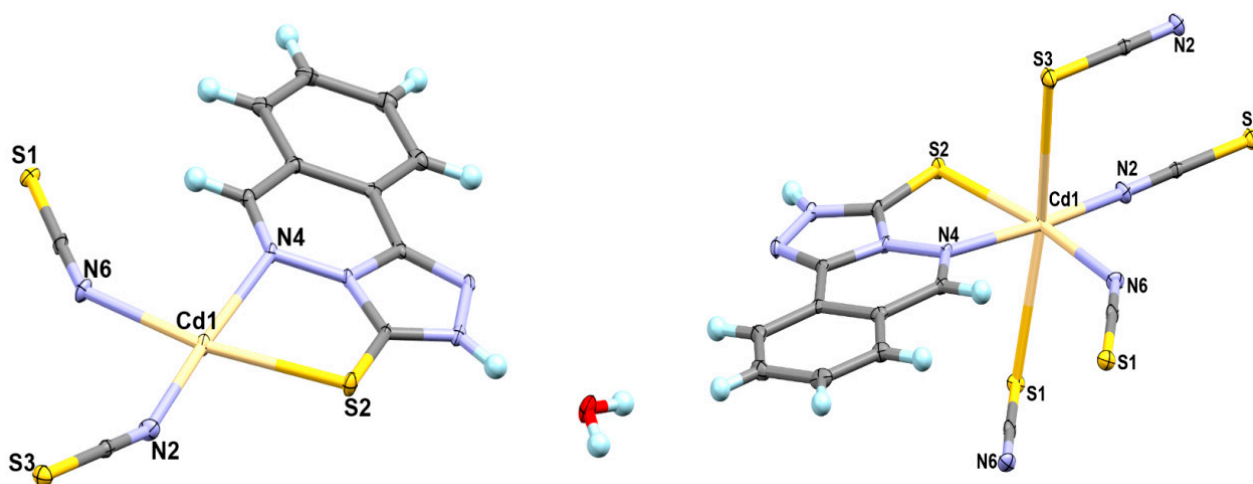


Figure 6. Asymmetric unit (left) and coordination sphere (right) with atom numbering for **2**.

Table 4. Bond distances (Å) and angles (°) for **2**.

Atoms	Distance	Atoms	Distance
Cd1-N2	2.256(4)	Cd1-S2	2.636(1)
Cd1-N6	2.338(4)	Cd1-S3	2.741(1)
Cd1-N4	2.480(3)	Cd1-S1	2.749(1)
Atoms	Angle	Atoms	Angle
N2-Cd1-N6	93.95(13)	N4-Cd1-S3	83.06(8)
N2-Cd1-N4	175.83(11)	S2-Cd1-S3	91.40(3)
N6-Cd1-N4	90.05(12)	N2-Cd1-S1	97.61(9)
N2-Cd1-S2	98.49(10)	N6-Cd1-S1	88.41(9)
N6-Cd1-S2	167.56(10)	N4-Cd1-S1	83.68(8)
N4-Cd1-S2	77.51(8)	S2-Cd1-S1	90.06(3)
N2-Cd1-S3	95.93(9)	S3-Cd1-S1	166.02(3)
N6-Cd1-S3	87.18(9)		

In this complex, the  $\mu(1,3)$  thiocyanate groups connect the Cd(II) centers, leading the 1D coordination polymer to extend along the crystallographic *b*-direction, as shown in the lower part of Figure 7. It is clear from the upper part of this figure that the crystal water molecules are located between the 1D chains and connecting the polymer chains via N-H...O, O-H...N, and O-H...S hydrogen bonding interactions, leading to a 2D supramolecular structure. A list of the hydrogen bond parameters is given in Table 5.

Table 5. The hydrogen bond parameters in **2**.

D-H...A	D-H (Å)	H...A (Å)	D...A (Å)	D-H...A(°)	Symm. Code
N3-H3A...O1	0.88	1.80	2.665(5)	166.0	
O1-H15...N6	0.73(7)	2.30(6)	3.005(5)	163(6)	<i>x,y,1+z</i>
O1-H16...S3	0.78(7)	2.67(7)	3.445(4)	168(6)	<i>x,y,1+z</i>

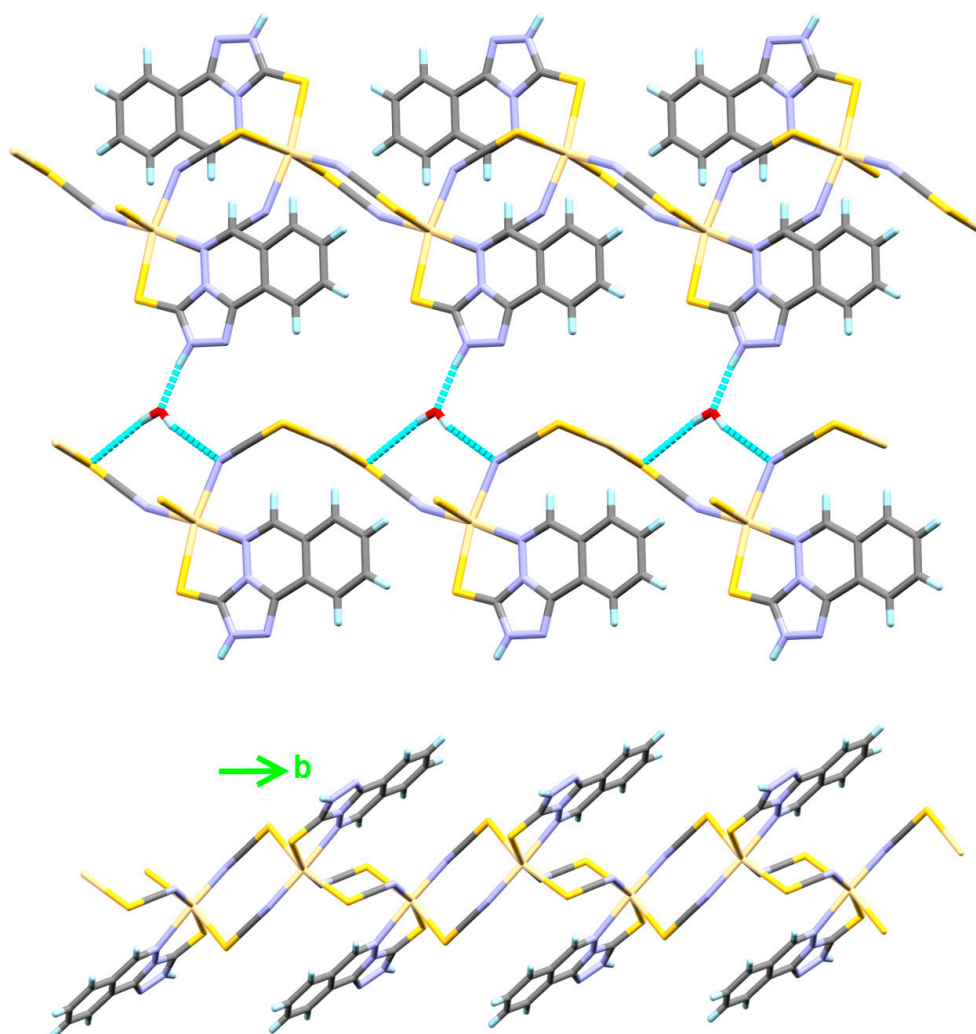


**Figure 7.** The 1D coordination polymer (**lower**) and the interconnected 1D chains via the hydrogen bonding interactions with the crystal water molecules leading to the 2D supramolecular structure.

In addition, the organic ligand units in the adjacent complex molecules are stacked together by the weak  $\pi$ - $\pi$  stacking interactions shown in Figure 8. The shortest contacts are shown in this figure as a turquoise dotted line with interaction distances of 3.342(6) Å, 3.240(6) Å, and 3.173(5) Å for C2...C9, C2...N3, and C2...N5, respectively.

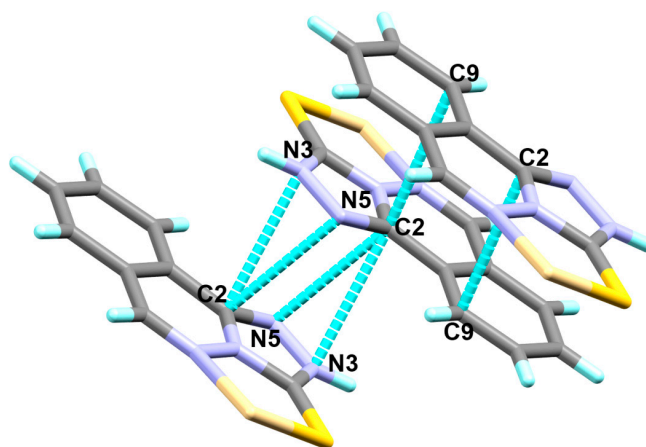


**Figure 8.** The most important  $\pi$ - $\pi$  stacking interactions among the stacked organic ligand units in **2**.

#### 4.1.3. $[\text{Cd}_3(\text{Hydralazine})_2(\text{H}_2\text{O})_2\text{Cl}_6]$ Complex; (3)

Similar to complexes **1** and **2**, the trinuclear  $[\text{Cd}_3(\text{Hydralazine})_2(\text{H}_2\text{O})_2\text{Cl}_6]$  complex (**3**) crystallized in the triclinic crystal system and P-1 space group. During the course of preparation, the ligand  $\text{HL}^{\text{OH}}$  underwent hydrolysis, affording the corresponding Cd(II)-hydralazine complex (**3**). In this case, there is an inversion center located at the Cd1 site splitting the trinuclear complex into two equivalent halves. Hence, the asymmetric unit represents half of the formula unit given above (Figure 9).

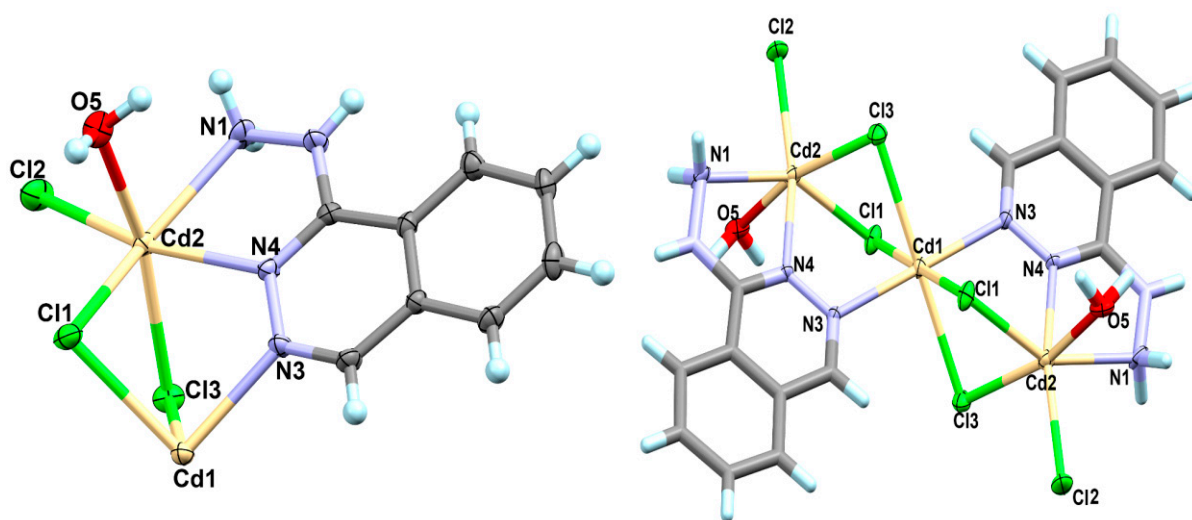


**Figure 9.** Asymmetric unit (**left**) and complete trinuclear complex unit (**right**) with atom numbering for **3**.

There are two crystallographically independent Cd atoms in this complex. The Cd2 is hexa-coordinated with one bidentate hydralazine ligand via two of its nitrogen atoms: one from the  $\text{NH}_2$  group with a Cd2-N1 distance of 2.432(5) Å and the other with one of the phthalazine nitrogen atoms with a Cd2-N4 distance of 2.318(5) Å. The coordination sphere of Cd2 is completed by one Cd2-O5 (2.427(5) Å) bond with a water molecule, one terminal Cd2-Cl2 bond (2.522(2) Å), and the two bridged Cd2-Cl1 (2.604(2) Å) and Cd2-Cl3 (2.657(2) Å) bonds. The bridging Cd2-Cl1 and Cd2-Cl3 bonds are slightly longer than the terminal Cd2-Cl2 bond (Table 6). The Cl1 and Cl3 atoms connect the two crystallographically independent Cd atoms with longer Cd1-Cl1 and Cd1-Cl3 bonds of 2.632(2) and 2.692(2) Å, respectively. The hexa-coordination environment of Cd1 is completed by two equivalent bonds with two *trans* hydralazine ligand units via N3 of the phthalazine moiety. The corresponding Cd1-N3 bond distance is 2.331(5) Å. Interestingly, the two symmetrically related *trans* Cd1-N3, Cd1-Cl1, and Cd1-Cl2 bonds make an angle of exactly 180.00°, which indicates the higher symmetrical coordination environment of Cd1 compared to Cd2. The phthalazine moiety could be considered as a NN-connector similar to that found in the  $[\text{Cd}(\text{Phtz})(\text{MeOH})(\text{N}_3)_2]_n$  complex [56]. The continuous shape measures of Cd1 and Cd2 are found to be 0.768 and 4.022 compared to the perfect octahedron while 17.135 and 7.797 compared to the perfect trigonal prism, respectively. Hence, the coordination geometry around both cadmium centers could be described as a distorted octahedral configuration. It is more distorted in the case of  $\text{CdN}_2\text{OCl}_3$  of Cd2 than  $\text{CdN}_2\text{Cl}_4$  of Cd1.

**Table 6.** Bond distances (Å) and angles (°) for **3**.

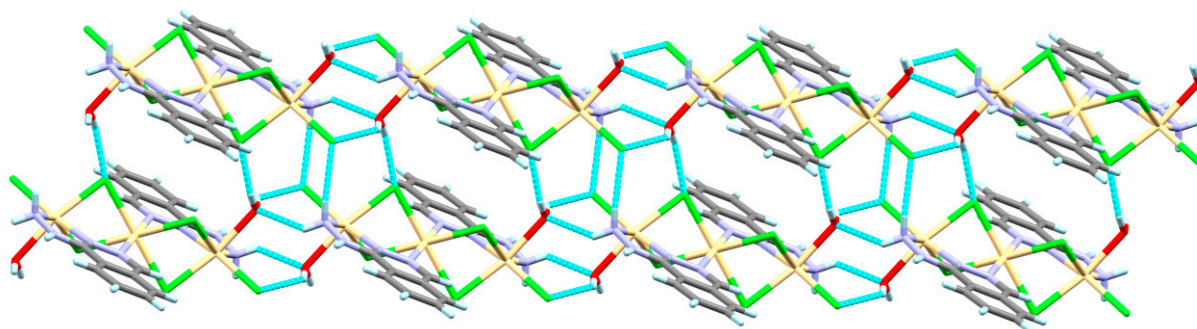
Atoms	Distance	Atoms	Distance
Cd1-Cl1	2.6320(17)	Cd2-N1	2.432(5)
Cd1-Cl1(I)	2.6320(17)	Cd2-Cl1	2.6039(17)
Cd1-Cl3(I)	2.6918(17)	Cd2-Cl2	2.5223(18)
Cd1-Cl3	2.6918(17)	Cd2-Cl3	2.6569(18)
Cd1-N3	2.331(5)	Cd2-N4	2.318(5)
Cd1-N3(I)	2.331(5)	Cd2-O5	2.427(5)
Atoms	Angle	Atoms	Angle
Cl1 <sup>1</sup> -Cd1-Cl1	180.00	O5-Cd2-N1	81.54(19)
Cl1-Cd1-Cl3 <sup>1</sup>	98.11(6)	O5-Cd2-Cl1	80.33(13)
Cl1 <sup>1</sup> -Cd1-Cl3	98.11(6)	O5-Cd2-Cl2	88.36(12)
Cl1 <sup>1</sup> -Cd1-Cl3 <sup>1</sup>	81.89(6)	O5-Cd2-Cl3	163.40(13)
Cl1-Cd1-Cl3	81.89(6)	N1-Cd2-Cl1	151.27(14)
Cl3-Cd1-Cl3 <sup>1</sup>	180.00(7)	N1-Cd2-Cl2	94.45(13)
N3 <sup>1</sup> -Cd1-Cl1	91.04(13)	N1-Cd2-Cl3	114.06(15)
N3 <sup>1</sup> -Cd1-Cl1 <sup>1</sup>	88.96(13)	Cl1-Cd2-Cl3	83.09(5)
N3-Cd1-Cl1 <sup>1</sup>	91.04(13)	Cl2-Cd2-Cl1	107.08(7)
N3-Cd1-Cl1	88.96(13)	Cl2-Cd2-Cl3	95.70(6)
N3-Cd1-Cl3	87.26(12)	N4-Cd2-N1	68.71(17)
N3 <sup>1</sup> -Cd1-Cl3 <sup>1</sup>	87.26(12)	N4-Cd2-Cl1	91.87(13)
N3 <sup>1</sup> -Cd1-Cl3	92.74(12)	N4-Cd2-Cl2	160.85(13)
N3-Cd1-Cl3 <sup>1</sup>	92.74(12)	N4-Cd2-Cl3	83.67(12)
N3 <sup>1</sup> -Cd1-N3	180.00	N4-Cd2-O5	97.70(16)

<sup>1</sup> 1-X,2-Y,1-Z.

It is clear that the structure comprised of discrete trinuclear Cd(II) complex and hence **3** could not be described as a coordination polymer. The trinuclear complex units are connected by a complicated set of N-H...Cl, N-H...O and O-H...Cl hydrogen bonding interactions with donor-acceptor distances of 3.464(7), 3.047(7) and 3.093(6)–3.227(5) Å, respectively (Table 7). A pictorial presentation of the two-dimensional hydrogen bonding network showing the molecular packing of the complex units is shown in Figure 10.

**Table 7.** The hydrogen bond parameters in **3**.

D-H...A	D-H (Å)	H...A (Å)	D...A (Å)	D-H...A(°)	Symm. Code
N1-H1A...Cl2	0.89	2.58	3.464(7)	173	1-x,2-y,-z
N1-H1B...O5	0.89	2.37	3.047(7)	133	2-x,2-y,-z
O5-H5A...Cl2	0.89	2.44	3.093(6)	131	2-x,2-y,-z
O5-H5B...Cl3	0.89	2.39	3.227(5)	157	1+x,y,z

**Figure 10.** The 2D hydrogen bonding network of **3**.

#### 4.2. Tautomerism and Proton Affinity of HL

It is well known that the hydrazonophthalazine ligands have a labile proton either located at the phthalazine ring *N*-atom or the hydrazone moiety. The X-ray structure of a very structurally related hydrazonophthalazine ligand was reported by us [15]. It was found that the labile proton favored the phthalazine *N*-site (N1 atom) rather than the hydrazone *N*-site. Based on this fact and the current DFT results (Table 8), the calculated total energies of both tautomers provided a strong demonstration in the case of ligand HL. The tautomer with a proton located at the phthalazine *N*-site (HL<sup>1</sup>) is energetically lower than the one with a proton at the hydrazone moiety (HL<sup>2</sup>) by 14.05 kcal/mol. Hence, the cationic ligand could be described as a protonated HL with an extra proton at the hydrazone moiety. The proton affinity of the hydrazone *N*-site was calculated to be  $-237.314$  kcal/mol.

**Table 8.** Energies and thermodynamic properties of the tautomeric forms of HL and its protonated form H<sub>2</sub>L<sup>+</sup>.

Parameter	HL <sup>1</sup>	HL <sup>2</sup>	H <sub>2</sub> L <sup>+</sup>
E	−1118.6190	−1118.5948	−1119.0100
ZPVE	0.2105	0.2086	0.2233
E <sub>corr</sub> <sup>a</sup>	−1118.4085	−1118.3861	−1118.7867
H	−1118.3933	−1118.3705	−1118.771078
G	−1118.4517	−1118.4308	−1118.830192

<sup>a</sup> E<sub>corr</sub> = E + ZPVE.

#### 4.3. Analysis of Molecular Packing

Hirshfeld surfaces mapped over  $d_{\text{norm}}$ , shape index (SI) and curvedness for the studied Cd(II) complexes are shown in Figure S8 (Supplementary data). Summary of the most important contacts and their percentages are shown in Figure 11. It is clear that the H...H interactions are common in all complexes where the percentages of these interactions comprised 20.9, 6.4 and 30.7% from the whole interactions occurred in complexes 1–3, respectively. The shortest H...H contacts are 2.220 Å (H1...H12), 2.424 Å (H11...H11) and 1.891 Å (H7...H5A), respectively. The H...H interactions are the strongest in complex 3, as clearly indicated from the decomposed fingerprint plot and  $d_{\text{norm}}$  map of this compound (Figures 12–14).

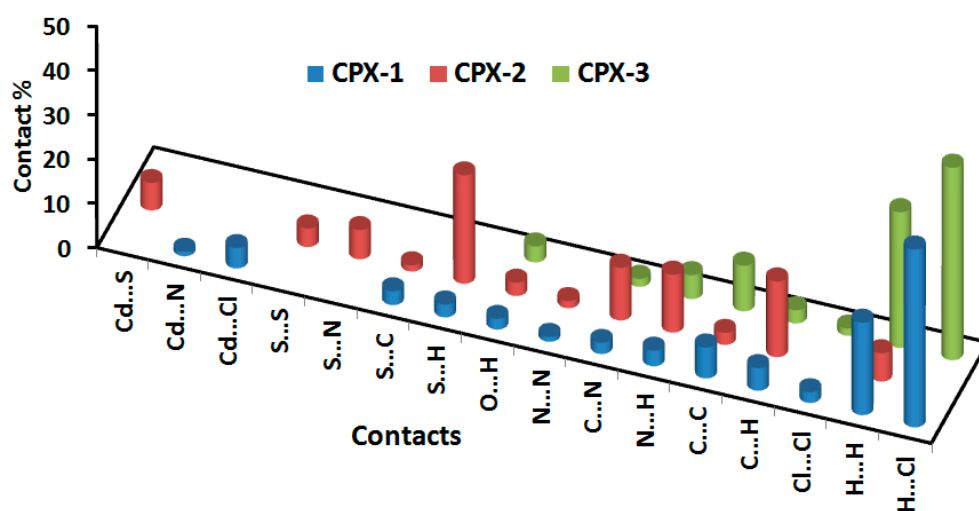


**Figure 11.** Summary of the intermolecular interactions and their percentages in the crystal structure of the studied Cd(II) complexes. Contacts with percentages less than 1% were omitted from this illustration for more clarity.

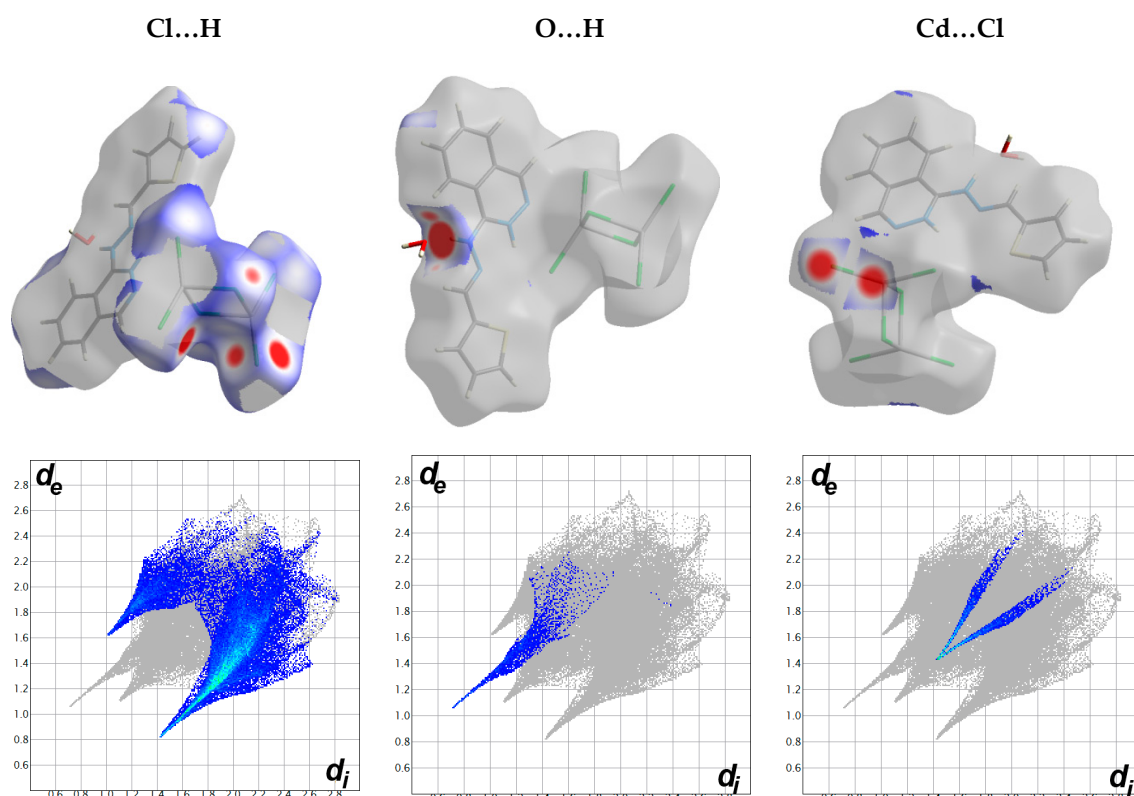


**Figure 12.** The decomposed fingerprint plots (lower) and  $d_{\text{norm}}$  maps (upper) of the most important contacts in complex 1.

In complex 1, the molecular packing of this complex is controlled mainly by strong O...H and Cl...H hydrogen bonds as well as Cd-Cl coordination interactions. All appeared as large red spots in the  $d_{\text{norm}}$  surfaces and sharp spikes in the fingerprint plots (Figure 12). The O...H, Cl...H and Cd-Cl contacts comprised 2.4%, 40.2%, and 4.6% from the whole fingerprint area of complex 1. The large red regions in the  $d_{\text{norm}}$  related to the Cd-Cl interactions indicating very well the polymeric structure of complex 1. In this complex, the molecular units of the organic ligand did not show any  $\pi$ - $\pi$  stacking interactions, as indicated from the shape index and curvedness maps of this complex (Supplementary Figure S8).

For complex 2, the packing of complex units is controlled by N...H (13.1%), O...H (3.0%), and S...H (24.5%) hydrogen bonds as well as Cd-S (6.2%) interactions. The presence of a large red spot in the  $d_{\text{norm}}$  map close to the Cd and S (SCN) atoms revealed that the molecular units are connected strongly by Cd-S coordination interactions, confirming the polymeric structure of this complex. All these interactions have also appeared as sharp spikes in the fingerprint plot indicating their significance (Figure 13). The N...H contacts appeared as a sharp spike at the lower right part of the fingerprint plot, indicating that these contacts occurred between the nitrogen atom of the thiocyanate groups inside the surface as hydrogen bond acceptor with the proton H15 from the crystal water molecule as hydrogen bond donor. The corresponding contact distance is 2.057 Å. The most important O...H hydrogen bonding interactions occurred between O1 of the crystal water as hydrogen bond acceptor and the N-H proton as hydrogen bond donor with contact distance of 1.678 Å for O1...H3A contact. The S...H interactions appeared as a sharper spike at the lower right side of the fingerprint plot compared to the spike at the lower left part of the same plot. As a result, the S...H interactions between the S-atom inside the surface and the hydrogen atoms outside the surface are more significant than the S...H interactions that occurred between the hydrogen atom inside the surface and the S-atom outside the surface. The corresponding S...H interactions are S3...H16 (2.480 Å) and S2...H8 (2.811 Å), respectively. The former belongs to the more polar O-H...S interaction, which is shorter than the less

polar C-H...S contact. Interestingly, the Hirshfeld analysis detected some short S...S contacts between two adjacent thiocyanate groups with a contact distance of 3.543 Å. Moreover, the packing of the complex units is controlled by some  $\pi$ - $\pi$  stacking interactions, as indicated by the relatively high contributions from the C...N (11.9%) and C...C (2.7%) interactions. It is worth noting that the shape index did not reveal this observation well as the stacking between the organic ligand units occurred partially between the ligand pairs, which are not fully stacked together (Supplementary Figure S8).

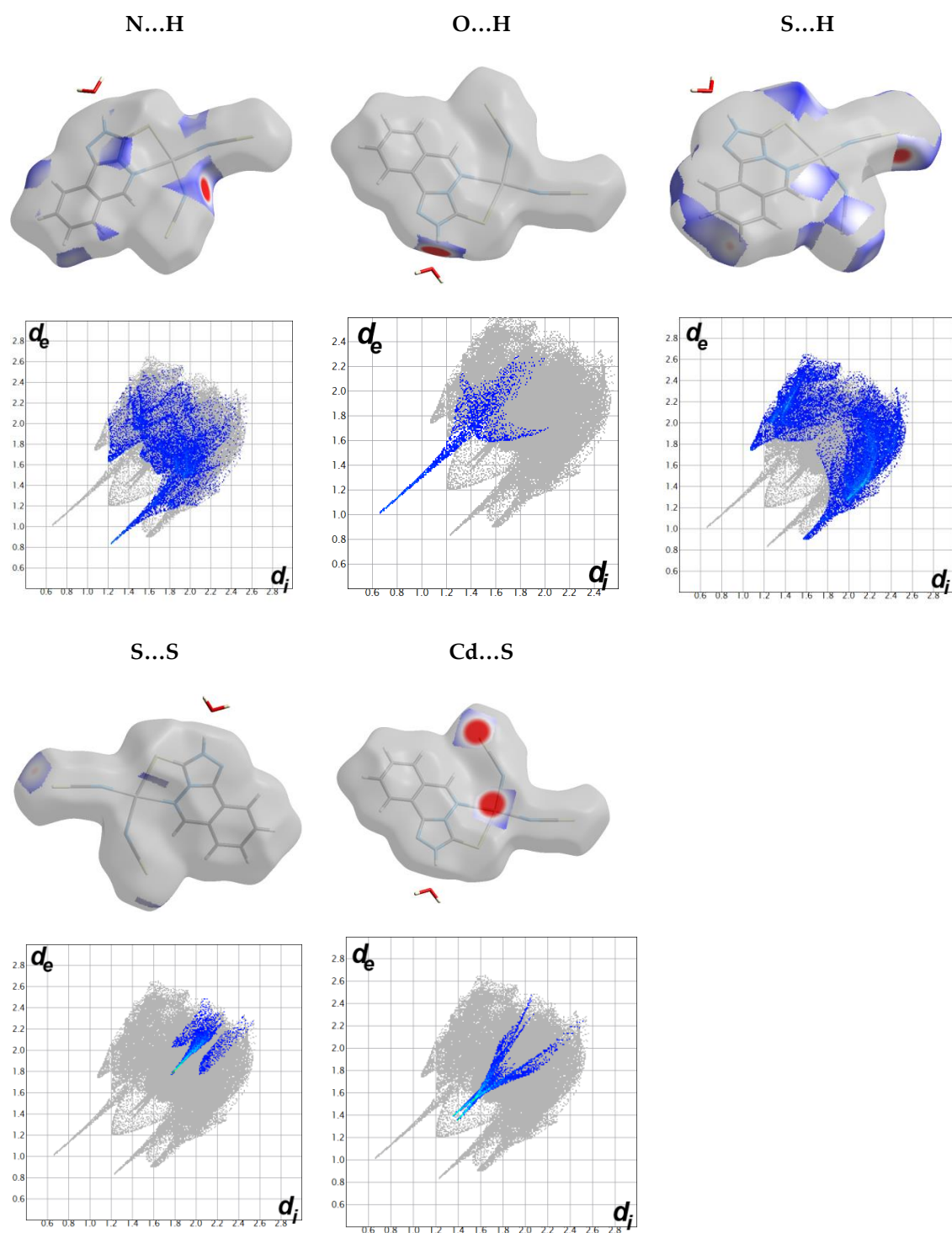


**Figure 13.** The decomposed fingerprint plots and  $d_{\text{norm}}$  maps of the most important contacts in complex 2.

The most important contacts as concluded from the Hirshfeld surface analysis shared in molecular packing of complex **3** are shown in Figure 14. It is clear that the Cl...H and O...H contacts are the most important ones. Many dark red spots in the decomposed  $d_{\text{norm}}$  map are corresponding to the Cl...H contacts. Moreover, two sharp spikes in the corresponding decomposed fingerprint plot provide strong evidence to support the importance of these intermolecular interactions. The percentage of the Cl...H interactions is 43.5% and the shortest contact distances are 2.302, 2.376, and 2.461 Å for the Cl3...H5B, Cl2...H5A, and Cl2...H1A, respectively. Pictorial presentation of O-H...Cl and N-H...Cl hydrogen bonding interactions is shown in Figure 15. Moreover, the O...H contacts appeared to be important. This occurred between one proton from the amino group of the hydrazine moiety as hydrogen bond donor and the oxygen atom from the water molecule as hydrogen bond acceptor. The shortest O...H contact distance is 2.292 Å for the O5...H1B which corresponds to the N1-H1B...O5 hydrogen bond.

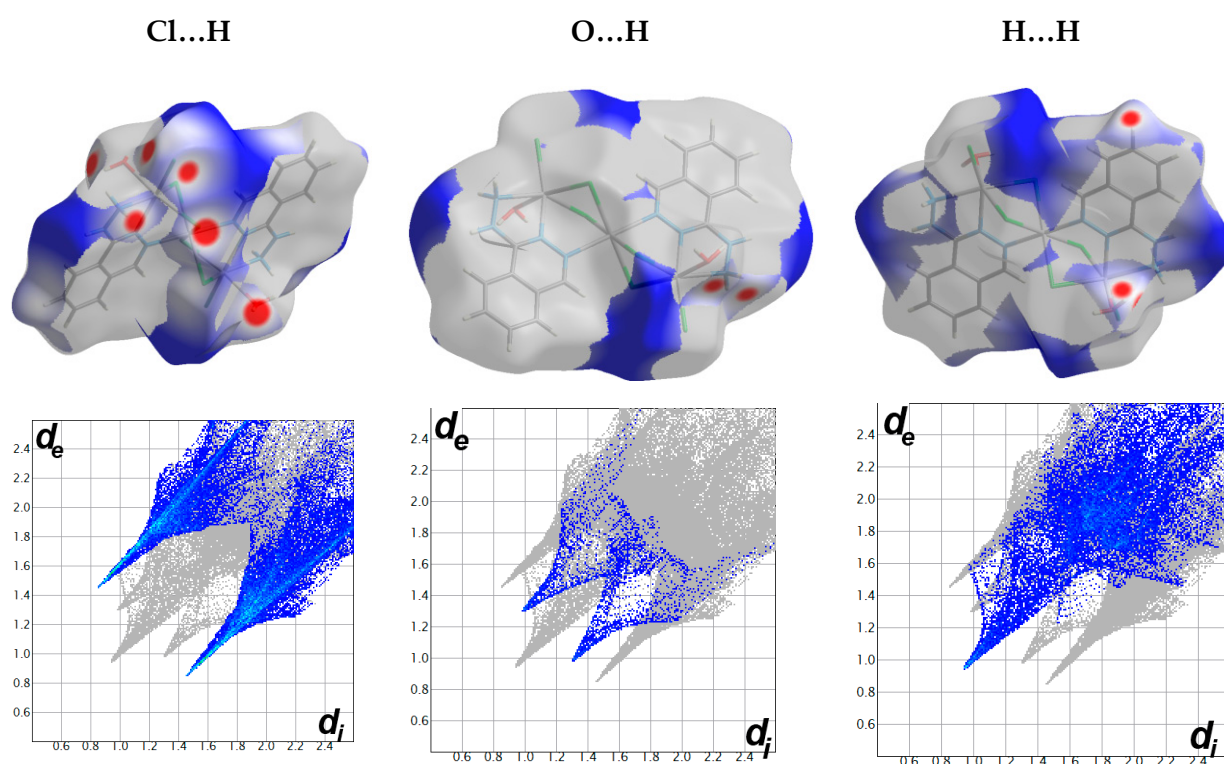


**Figure 14.** The decomposed fingerprint plots (**lower**) and  $d_{\text{norm}}$  maps (**upper**) of the most important contacts in complex **3**.

Another interesting feature of molecular packing is clearly seen from the shape index map, which is the presence of complementary red/blue triangles corresponding to the  $\pi$ - $\pi$  stacking interactions between the almost parallel stacked phthalazine rings with relatively longer C...C contacts compared to complex **2** (Figure 16). The shortest C...C contact distances range from 3.452 to 3.547 Å, corresponding to the C5...C9 contacts.

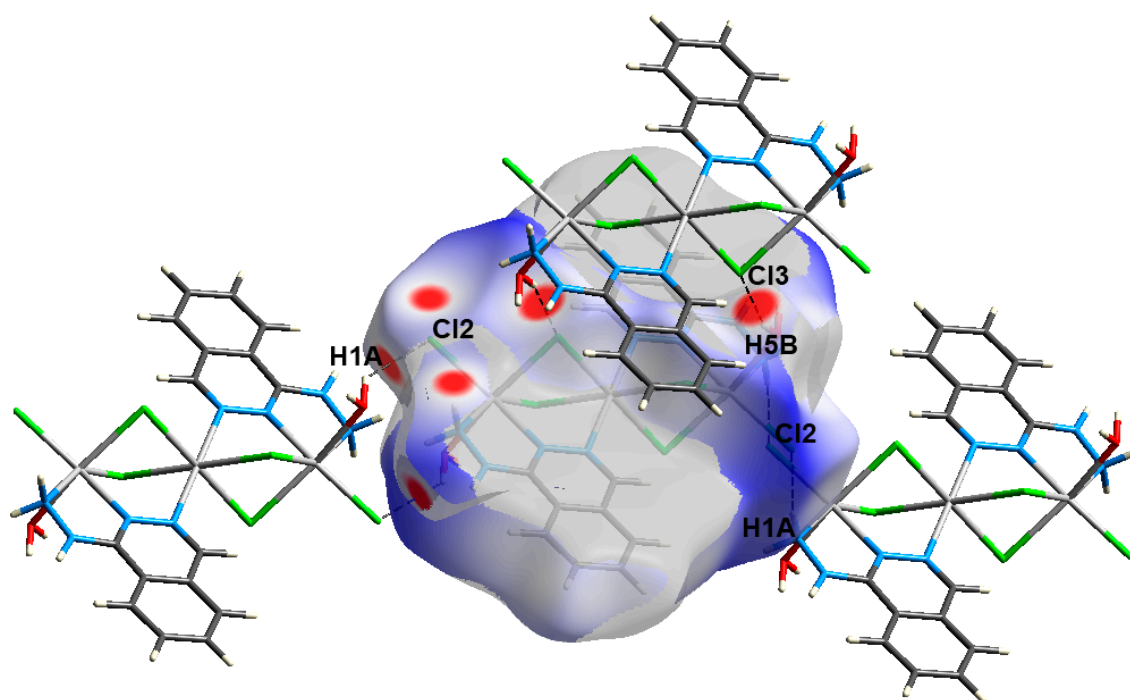


**Figure 15.** The Hirshfeld surface showing the molecular packing diagram showing the Cl...H hydrogen bonds in complex 3.

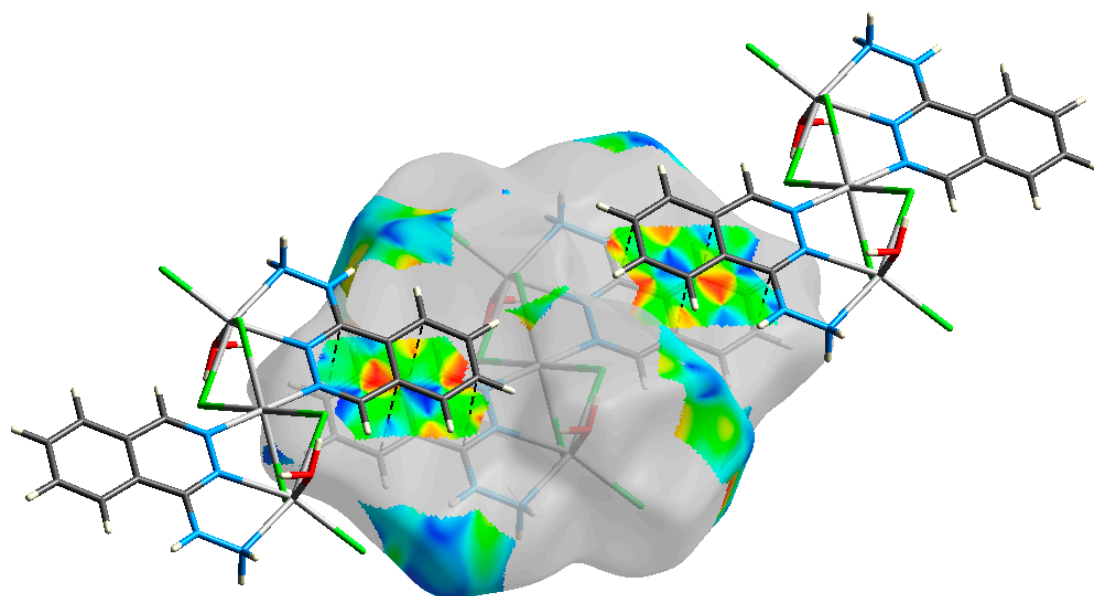


**Figure 16.** The red/blue triangles in the shape index revealed the weak  $\pi$ - $\pi$  stacking interactions between the almost parallel phthalazine moieties in complex 3.

## 5. Conclusions

Reactions of two new hydrazonephthalazines (HL and HL<sup>OH</sup>) with CdCl<sub>2</sub> afforded two 1D polymeric and one trinuclear Cd(II) complex depending on the reaction conditions. The molecular and supramolecular structure aspects of these Cd(II) complexes were investigated using single crystal X-ray diffraction and Hirshfeld calculations. The [Cd(H<sub>2</sub>L)Cl<sub>3</sub>]<sub>n</sub>\*(H<sub>2</sub>O)<sub>n</sub>, **1**, and [Cd(TPT)(SCN)<sub>2</sub>]<sub>n</sub>\*(H<sub>2</sub>O)<sub>n</sub>, **2**, 1D polymers comprised one symmetrically independent Cd(II) connected by bridged chloride and  $\mu(1,3)$  thiocyanate ions, respectively, while [Cd<sub>3</sub>(Hydralazine)<sub>2</sub>(H<sub>2</sub>O)<sub>2</sub>Cl<sub>6</sub>], **3**, is a trinuclear with two symmetrically independent Cd(II) ions having CdN<sub>2</sub>Cl<sub>4</sub> and CdN<sub>2</sub>OCl<sub>3</sub> coordination spheres

for Cd1 and Cd2, respectively. In complex **1**, the protonated HL is acting as a cationic monodentate ligand coordinating the Cd(II) ion via one nitrogen atom from the phthalazine moiety and with an extra proton at one of the hydrazone nitrogen atoms. During the course of the preparation of complexes **2** and **3**, the HL underwent cyclization to the triazolophthalazine (TPT) while the HL<sup>OH</sup> underwent hydrolysis to hydralazine, respectively. Hirshfeld analysis was used to quantify all interactions controlling the molecular packing of the studied Cd(II) complexes.

**Supplementary Materials:** The following are available online at <https://www.mdpi.com/article/10.3390/cryst11070823/s1>, Figure S1: <sup>1</sup>H-NMR spectra of HL; Figure S2: <sup>13</sup>C-NMR spectra of HL; Figure S3: <sup>1</sup>H-NMR spectra of HL<sup>OH</sup>; Figure S4: <sup>13</sup>C-NMR spectra of HL<sup>OH</sup>; Figure S5: FTIR spectra of [Cd(H<sub>2</sub>L)Cl<sub>3</sub>]<sub>n</sub>·H<sub>2</sub>O; **1**; Figure S6: FTIR spectra of [Cd(TPT)(SCN)<sub>2</sub>]<sub>n</sub>·H<sub>2</sub>O; **2**; Figure S7: FTIR spectra of [Cd<sub>3</sub>(Hydralazine)<sub>2</sub>(H<sub>2</sub>O)<sub>2</sub>Cl<sub>6</sub>]<sub>n</sub>; **1**; Figure S8 Hirshfeld d<sub>norm</sub> (−0.2–2.0), shape index (SI) and curvedness surfaces of the studied complexes.

**Author Contributions:** The work was designed and supervised by S.M.S. X-ray structure analyses were performed by S.M.S. Computational calculations as well as the synthesis of complex was carried out by S.M.S. and R.A.M.; A.E.-F. and H.H.A.-R. carried out the preparations of the organic ligands and their analyses. All authors contributed to the first draft and the final version. All authors have read and agreed to the published version of the manuscript.

**Funding:** Deanship of Scientific Research at King Saud University funded this research, grant number RG-1441-365, Saudi Arabia.

**Institutional Review Board Statement:** Not applicable.

**Informed Consent Statement:** Not applicable.

**Data Availability Statement:** The data presented in this study are not available on request from the corresponding author.

**Acknowledgments:** The authors extend their thanks to the Deanship of Scientific Research at King Saud University for funding this work through research group no. (RG-1441-365, Saudi Arabia).

**Conflicts of Interest:** The authors declare no conflict of interest.

## References

1. Liu, D.; Gong, G.; Wei, C.; Jin, X.; Quan, Z. Synthesis and anti-inflammatory activity evaluation of a novel series of 6-phenoxy-[1,2,4]triazolo[3,4-a]phthalazine-3-carboxamide derivatives. *Bioorg. Med. Chem. Lett.* **2016**, *26*, 1576–1579. [[CrossRef](#)]
2. El-Shamy, I.E.; Abdel-Mohsen, A.M.; Alsheikh, A.A.; Fouda, M.M.G.; Al-Deyab, S.S.; El-Hashash, M.A.; Jancar, J. Synthesis, biological, anti-inflammatory activities and quantum chemical calculation of some [4-(2,4,6-trimethylphenyl)-1(2H)-oxo-phthalazin-2yl] acetic acid hydrazide derivatives. *Dye. Pigment.* **2015**, *113*, 357–371. [[CrossRef](#)]
3. Behalo, M.S. An efficient one-pot catalyzed synthesis of 2,5-disubstituted-1,3,4-oxadiazoles and evaluation of their antimicrobial activities. *RSC Adv.* **2016**, *6*, 103132–103136. [[CrossRef](#)]
4. Hollo, B.; Magyari, J.; Radovanovic, V. Ž.; Vučkovic, G.; Tomic, Z.D.; Szilágyi, I.M.; Pokol, G.; Szécsény, K.M. Synthesis, characterisation and antimicrobial activity of bis(phthalazine-1-hydrazone)-2,6-diacetylpyridine and its complexes with Co<sup>III</sup>, Ni<sup>II</sup>, Cu<sup>II</sup> and Zn<sup>II</sup>. *Polyhedron* **2014**, *80*, 142–150. [[CrossRef](#)]
5. Issac, Y.A.; El-Karim, I.G.; Donia, S.G.; Behalo, M.S. Novel synthesis of phthalazine derivatives as antimicrobial agents. *Sulfur Lett.* **2002**, *25*, 183–190. [[CrossRef](#)]
6. Zhang, Q.R.; Xue, D.Q.; He, P.; Shao, K.P.; Chen, P.J.; Gu, Y.F.; Ren, J.L.; Shan, L.H.; Liu, H.M. Synthesis and antimicrobial activities of novel 1,2,4-triazolo [3,4-a] phthalazine derivatives. *Bioorg. Med. Chem. Lett.* **2014**, *24*, 1236–1238. [[CrossRef](#)] [[PubMed](#)]
7. Glišić, B.Đ.; Senerovic, L.; Comba, P.; Wadepohl, H.; Veselinovic, A.; Milivojevic, D.R.; Djuran, M.I.; Runic, J.N. Silver(I) complexes with phthalazine and quinazoline as effective agents against pathogenic *Pseudomonas aeruginosa* strains. *J. Inorg. Biochem.* **2016**, *155*, 115–128. [[CrossRef](#)]
8. El-hashash, M.A.; Soliman, A.Y.; EL-Sham, I.E. Synthesis and antimicrobial evaluation of some annelated phthalazine derivatives and acyclo C-nucleosides from 1-chloro-4-(2,4,6-trimethylphenyl) phthalazine precursor. *Turk. J. Chem.* **2012**, *36*, 347–366.
9. Sagar, P.; Kumar, V.; Suresh, L.; Chandramouli, G.V.P. Ionic liquid catalysed multicomponent synthesis, antifungal activity, docking studies and in silico ADMET properties of novel fused Chromeno-Pyrazolo-Phthalazine derivatives. *J. Saudi Chem. Soc.* **2017**, *21*, 306–314. [[CrossRef](#)]

10. Savinia, L.; Chiasserinia, L.; Travaglia, V.; Pellerano, C.; Novellino, E.; Cosentinoc, S.; Pisano, M.B. New  $\alpha$ -(N)-heterocyclchydrazones: Evaluation of anticancer, anti-HIV and antimicrobial activity. *Eur. J. Med. Chem.* **2004**, *39*, 113–122. [[CrossRef](#)]
11. El-Helby, A.A.; Ayyad, R.R.; Sakr, H.M.; Abdelrahim, A.S.; El-Adl, K.; Sherbiny, F.S.; Eissa, I.H.; Khalifa, M.M. Design, synthesis, molecular modeling and biological evaluation of novel 2,3-dihydrophthalazine-1,4-dione derivatives as potential anticonvulsant agents. *J. Mol. Struct.* **2017**, *1130*, 333–351. [[CrossRef](#)]
12. Wasfy, A.F.; Behalo, M.S.; Aly, A.A.; Sobhi, N.M. An efficient synthesis of some new 1, 4-disubstituted phthalazine derivatives and their anticancer activity. *Der PharmaChemica* **2013**, *5*, 82–96.
13. Amin, K.M.; Barsoum, F.F.; Awadallah, F.M.; Mohamed, N.E. Identification of new potent phthalazine derivatives with VEGFR-2 and EGFR kinase inhibitory activity. *Eur. J. Med. Chem.* **2016**, *123*, 191–201. [[CrossRef](#)] [[PubMed](#)]
14. Eldehna, W.M.; Abou-Seri, S.M.; El Kerdawy, A.M.; Ayyad, R.R.; Hamdy, A.M.; Ghabbour, H.A.; Ali, M.M.; Abou El Ella, D.A. Increasing the binding affinity of VEGFR-2 inhibitors by extending their hydrophobic interaction with the active site: Design, synthesis and biological evaluation of 1-substituted-4-(4-methoxybenzyl)phthalazine derivatives. *Eur. J. Med. Chem.* **2016**, *113*, 50–62. [[CrossRef](#)] [[PubMed](#)]
15. Soliman, S.M.; Albering, J.H.; Farooq, M.; Wadaan, M.A.M.; El-Faham, A. Synthesis, structural and biological studies of two new Co (III) complexes with tridentate hydrazone ligand derived from the antihypertensive drug hydralazine. *Inorg. Chim. Acta* **2017**, *466*, 16–29. [[CrossRef](#)]
16. Sousa, C.; Freire, C.; de Castro, B. Synthesis and Characterization of Benzo-15-Crown-5 Ethers with Appended N<sub>2</sub>O Schiff Bases. *Molecules* **2003**, *8*, 894–900. [[CrossRef](#)]
17. Shahsavani, M.B.; Ahmadi, S.; Aseman, M.D.; Nabavizadeh, S.M.; Rashidi, M.; Asadi, Z.; Erfani, N.; Ghasemi, A.; Saboury, A.A.; Niazi, A.; et al. Anticancer activity assessment of two novel binuclear platinum (II) complexes. *J. Photochem. Photobiol. B Biol.* **2016**, *161*, 345–354. [[CrossRef](#)]
18. Tomek, P.; Palmer, B.D.; Flanagan, J.U.; Sun, C.; Raven, E.L.; Ching, L. Discovery and evaluation of inhibitors to the immunosuppressive enzyme indoleamine 2,3-dioxygenase 1 (IDO1): Probing the active site-inhibitor interactions. *Eur. J. Med. Chem.* **2017**, *126*, 983–996. [[CrossRef](#)]
19. Xue, D.Q.; Zhang, X.Y.; Wang, C.J.; Ma, L.Y.; Shao, K.P.; Chen, P.J.; Gu, Y.F.; Zhang, X.S.; Wang, C.F.; Ji, C.H.; et al. Synthesis and anticancer activities of novel 1,2,4-triazolo[3,4-a]phthalazine derivatives. *Eur. J. Med. Chem.* **2014**, *85*, 235–244. [[CrossRef](#)]
20. Abou-Seri, S.M.; Eldehna, W.M.; Ali, M.M.; Abou El Ella, D.A. 1-Piperazinylphthalazines as potential VEGFR-2 inhibitors and anticancer agents: Synthesis and in vitro biological evaluation. *Eur. J. Med. Chem.* **2016**, *107*, 165–179. [[CrossRef](#)]
21. Subramanian, G.; Babu Rajeev, C.P.; Mohan, C.D.; Sinha, A.; Chu, T.T.; Anusha, S.; Ximei, H.; Fuchs, J.E.; Bender, A.; Rangappa, K.S.; et al. Synthesis and in vitro evaluation of hydrazinyl phthalazines against malaria parasite, Plasmodium falciparum. *Bioorg. Med. Chem. Lett.* **2016**, *15*, 3300–3306. [[CrossRef](#)]
22. Sullivan, D.A.; Palenik, G.J. Binuclear Complexes. Synthesis and Characterization of the Binuclear Ligand 1,4-Dihydrazinophthalazine Bis(2'-pyridinecarboxaldimine) and the Nickel Complex p-Chloro-tetraaqua[1,4-dihydrazinophthalazine bis(2'-pyridinecarboxaldimine)]dinickel(II) Chloride Dihydrate. *Inorg. Chem.* **1977**, *16*, 1127–1133.
23. Lee, J.J.; Choi, Y.W.; You, G.R.; Lee, S.Y.; Kim, C. A phthalazine-based two-in-one chromogenic receptor for detecting Co<sup>2+</sup> and Cu<sup>2+</sup> in an aqueous environment. *Dalton Trans.* **2015**, *44*, 13305–13314. [[CrossRef](#)] [[PubMed](#)]
24. Molina, P.; Tárraga, A.; Otón, F. Imidazole derivatives: A comprehensive survey of their recognition properties. *Org. Biomol. Chem.* **2012**, *10*, 1711–1724. [[CrossRef](#)] [[PubMed](#)]
25. Shibutani, M.; Mitsumori, K.; Niho, N.; Satoh, S.; Hiratsuka, H.; Satoh, M.; Sumiyoshi, M.; Nishijima, M.; Katsuki, Y.; Suzuki, J.; et al. Assessment of renal toxicity by analysis of regeneration of tubular epithelium in rats given low-dose cadmium chloride or cadmium-polluted rice for 22 months. *Arch. Toxicol.* **2000**, *74*, 571–577. [[CrossRef](#)]
26. Chen, L.; Lei, L.; Jin, T.; Nordberg, M.; Nordberg, G.F. Plasma Metallothionein Antibody, Urinary Cadmium, and Renal Dysfunction in a Chinese Type 2 Diabetic Population. *Diabetes Care* **2006**, *29*, 2682–2687. [[CrossRef](#)] [[PubMed](#)]
27. Antonio, M.T.; Corredor, L.; Leret, M.L. Study of the activity of several brain enzymes like markers of the neurotoxicity induced by perinatal exposure to lead and/or cadmium. *Toxicol. Lett.* **2003**, *143*, 331–340. [[CrossRef](#)]
28. Rikans, L.E.; Yamano, T. Mechanisms of cadmium-mediated acute hepatotoxicity. *J. Biochem. Mol. Toxicol.* **2000**, *14*, 110–117. [[CrossRef](#)]
29. Lane, T.W.; Morel, F.M.M. A biological function for cadmium in marine diatoms. *Proc. Natl. Acad. Sci. USA* **2000**, *97*, 4627–4631. [[CrossRef](#)]
30. Gong, Y.-Q.; Fan, J.; Wang, R.-H.; Zhou, Y.-F.; Yuan, D.-Q.; Hong, M.-C. Syntheses, crystal structures and photoluminescence of two Cd(II) coordination polymers derived from a flexible bipyridyl ligand. *J. Mol. Struct.* **2004**, *705*, 29–34. [[CrossRef](#)]
31. Li, W.; Evans, O.-R.; Xiong, R.-G.; Wang, Z. Supramolecular Engineering of Chiral and Acentric 2D Networks. Synthesis, Structures, and Second-Order Nonlinear Optical Properties of Bis(nicotinato)zinc and Bis[3-[2-(4-pyridyl)ethenyl]benzoato]cadmium. *J. Am. Chem. Soc.* **1998**, *120*, 13272–13273.
32. Lin, W.; Wang, Z.; Ma, L. A Novel Octupolar Metal–Organic NLO Material Based on a Chiral 2D Coordination Network. *J. Am. Chem. Soc.* **1999**, *121*, 11249–11250. [[CrossRef](#)]
33. Chen, Y.-B.; Zhang, J.; Cheng, J.-K.; Kang, Y.; Li, Z.-J.; Yao, Y.-G. 1D chain structure, NLO and luminescence properties of [Zn<sub>2</sub>(bpp)(pht)<sub>2</sub>]. *Inorg. Chem. Commun.* **2004**, *7*, 1139–1141. [[CrossRef](#)]

34. Cooke, N.H.C.; Viavattene, R.L.; Eksteen, R.; Wong, W.S.; Davies, G.; Karger, B.L. Use of metal ions for selective separations in high-performance liquid chromatography. *J. Chromatogr.* **1978**, *149*, 391–415. [[CrossRef](#)]
35. Le Page, J.N.; Lindner, W.; Davies, G.; Seitz, D.E.; Karger, B.L. Resolution of the optical isomers of dansyl amino acids by reversed phase liquid chromatography with optically active metal chelate additives. *Anal. Chem.* **1979**, *51*, 433–435. [[CrossRef](#)]
36. Lindner, W. HPLC-Enantiomertrennung an gebundenen chiralen Phasen. *Nat. Schaften* **1980**, *67*, 354–356. [[CrossRef](#)]
37. Hashemi, L.; Hosseinfard, M.; Amani, V.; Morsali, A.J. Sonochemical Synthesis of Two New Nano-structured Cadmium (II) Supramolecular Complexes. *Inorg. Organomet. Polym.* **2013**, *23*, 519–524. [[CrossRef](#)]
38. Mlowe, S.; Lewis, D.J.; Malik, M.A.; Raftery, J.; Mubofu, E.B.; O'Brien, P.; Revaprasadu, N. Bis(piperidinedithiocarbamate)pyridine cadmium(II) as a single-source precursor for the synthesis of CdS nanoparticles and aerosol-assisted chemical vapour deposition (AACVD) of CdS thin films. *New J. Chem.* **2014**, *38*, 6073–6080. [[CrossRef](#)]
39. Mirtamizdoust, B.; Hanifehpour, Y.; Behzadfar, E.; Sadeghi-Roodsari, M.; Jung, J.H.; Joo, S.W. A novel nano-structured three-dimensional supramolecular metal-organic framework for cadmium (II): A new precursor for producing nano cadmium oxide. *J. Mol. Struct.* **2020**, *1201*, 127191. [[CrossRef](#)]
40. Hanifehpour, Y.; Dadashi, J.; Mirtamizdoust, B. Ultrasound-Assisted Synthesis and Crystal Structure of Novel 2D Cd (II) Metal–Organic Coordination Polymer with Nitrite End Stop Ligand as a Precursor for Preparation of CdO Nanoparticles. *Crystals* **2021**, *11*, 197. [[CrossRef](#)]
41. Zhang, Z.Y.; Bi, C.F.; Fan, Y.H.; Yan, X.C.; Zhang, X.; Zhang, P.F.; Huang, G.M. Synthesis, crystal structures, luminescent properties, theoretical calculation, and DNA interaction of the cadmium (II) and lead (II) complexes with *o*-aminobenzoic acid and 1, 10-phenanthroline. *Russ. J. Coord. Chem.* **2015**, *41*, 274–284. [[CrossRef](#)]
42. Jana, S.K.; Mandal, A.K.; Seth, S.K.; Puschmann, H.; Hossain, M.; Dalai, S. Synthesis, Characterization and Crystal Structure of a New 3D Cadmium(II) Coordination Polymer: Binding Interaction with DNA and Double Stranded RNA. *J. Inorg. Organomet. Polym.* **2016**, *26*, 806–818. [[CrossRef](#)]
43. Zianna, A.; Ristović, M.Š.; Psomas, G.; Hatzidimitriou, A.; Coutouli-Argyropoulou, E.; Lalia-Kantouri, M. Cadmium(II) complexes of 5-bromo-salicylaldehyde and  $\alpha$ -diimines: Synthesis, structure and interaction with calf-thymus DNA and albumins. *Polyhedron* **2016**, *107*, 136–147. [[CrossRef](#)]
44. Wazeer, M.I.M.; Isab, A.A.; Fettouhi, M. New cadmium chloride complexes with imidazolidine-2-thione and its derivatives: X-ray structures, solid state and solution NMR and antimicrobial activity studies. *Polyhedron* **2007**, *26*, 1725–1730. [[CrossRef](#)]
45. Ruiz, M.; Perelló, L.; Server-Carrió, J.; Ortiz, R.; García-Granda, S.; Díaz, M.R.; Cantón, E. Cinoxacin complexes with divalent metal ions. Spectroscopic characterization. Crystal structure of a new dinuclear Cd(II) complex having two chelate-bridging carboxylate groups. Antibacterial studies. *J. Inorg. Biochem.* **1998**, *69*, 231–239. [[CrossRef](#)]
46. Dubler, E.; Gyr, E. New metal complexes of the antitumor drug 6-mercaptopurine. Syntheses and x-ray structural characterizations of dichloro(6-mercaptopurinium)copper(I), dichlorotetrakis(6-mercaptopurine)cadmium(II), and bis(6-mercaptopurinato)cadmium(II) hydrate. *Inorg. Chem.* **1988**, *27*, 1466–1473. [[CrossRef](#)]
47. Perez, J.M.; Cerrillo, V.; Matesanz, A.I.; Millan, J.M.; Navarro, P.; Alonso, C.; Souza, P. DNA Interstrand Cross-Linking Efficiency and Cytotoxic Activity of Novel Cadmium(II)–Thiocarbodiazone Complexes. *ChemBioChem* **2001**, *2*, 119–123. [[CrossRef](#)]
48. Ignatius, I.C.; Rajathi, S.; Kirubavathi, K.; Selvaraju, K. Synthesis, crystal growth and characterization of novel semiorganic nonlinear optical crystal: Dichloro(beta-alanine)cadmium(II). *Optik* **2014**, *125*, 5144–5147. [[CrossRef](#)]
49. Saghatforoush, L.; Khoshtarkib, Z.; Keypour, H.; Hakimi, M. Mononuclear, tetranuclear and polymeric cadmium(II) complexes with the 3,6-bis(2-pyridyl)-1,2,4,5-tetrazine ligand: Synthesis, crystal structure, spectroscopic and DFT studies. *Polyhedron* **2016**, *119*, 160–174. [[CrossRef](#)]
50. Wang, W.; Qiao, J.; Wang, L.; Duan, L.; Zhang, D.; Yang, W.; Qiu, Y. Synthesis, Structures, and Optical Properties of Cadmium Iodide/Phenethylamine Hybrid Materials with Controlled Structures and Emissions. *Inorg.Chem.* **2007**, *46*, 10252–10260. [[CrossRef](#)]
51. Biswas, F.B.; Roy, T.G.; Rahman, A.; Emran, T.B. An in vitro antibacterial and antifungal effects of cadmium (II) complexes of hexamethyltetraazacyclotetradecadiene and isomers of its saturated analogue *Asian Pac. J. Trop. Med.* **2014**, *7*, S534–S539.
52. Yi, X.C.; Huang, M.X.; Qi, Y.; Gao, E.Q. Synthesis, structure, luminescence and catalytic properties of cadmium(II) coordination polymers with 9H-carbazole-2,7-dicarboxylic acid. *Dalton Trans.* **2014**, *43*, 3691–3697. [[CrossRef](#)] [[PubMed](#)]
53. Jia, W.G.; Li, D.D.; Gu, C.; Dai, Y.C.; Zhou, Y.H.; Yuan, G.; Sheng, E.H. Two cadmium(II) complexes with oxazoline-based ligands as effective catalysts for C–N cross-coupling reactions. *Inorg. Chim. Acta* **2015**, *427*, 226–231. [[CrossRef](#)]
54. Tronic, T.A. Copper (I) Cyanide Networks: Synthesis, Luminescence Behavior and Thermal Analysis. Part 1. Diimine Ligands. *Inorg. Chem.* **2007**, *46*, 8897–8912. [[CrossRef](#)]
55. Abu-Youssef, M.A.M.; Escuer, A.; Langer, V. New Polymeric Manganese Azide Derivatives with Quinazoline. *Eur. J. Inorg. Chem.* **2005**, *2005*, 4659–4664. [[CrossRef](#)]
56. Machura, B.; Nawrot, I.; Kruszynski, R.; Dulski, M. Syntheses, structures, thermal and luminescent properties of cadmium(II) complexes based on quinazoline and phthalazine. *Polyhedron* **2013**, *54*, 272–284. [[CrossRef](#)]
57. Soliman, S.M.; El-Faham, A. Low temperature X-ray structure analyses combined with NBO studies of a new heteroleptic octa-coordinated Holmium(III) complex with *N,N,N*-tridentate hydrazono-phthalazine-type ligand. *J. Mol. Struct.* **2018**, *1157*, 222–229. [[CrossRef](#)]

58. Soliman, S.M.; Albring, J.H.; El-Faham, A. Cu(II)-promoted cyclization of hydrazonophthalazine to triazolophthalazine; Synthesis and structure diversity of six novel Cu(II)-triazolophthalazine complexes. *Appl. Organomet. Chem.* **2019**, *33*, e4992. [[CrossRef](#)]
59. Roy, S.; Bauzá, A.; Frontera, A.; Chattopadhyay, S. A combined experimental and theoretical study on the synthesis and characterization of two new dinuclear cadmium (II) Schiff base complexes with selenocyanate- $\kappa$ -Se. *Inorg. Chim. Acta* **2016**, *453*, 51–61. [[CrossRef](#)]
60. Frisch, M.J.; Trucks, G.W.; Schlegel, H.B.; Scuseria, G.E.; Robb, M.A.; Cheeseman, J.R.; Scalmani, G.; Barone, V.; Mennucci, B.; Petersson, G.A.; et al. *GAUSSIAN 09.Revision A02*; Gaussian Inc.: Wallingford, CT, USA, 2009.
61. Sheldrick, G.M. *Program for Empirical Absorption Correction of Area Detector Data*; University of Göttingen: Göttingen, Germany, 1996.
62. Sheldrick, G.M. SHELXT-Integrated space-group and crystal-structure determination. *Acta Cryst. A* **2015**, *71*, 3–8. [[CrossRef](#)]
63. Spek, A.L. Structure validation in chemical crystallography. *Acta Cryst. D* **2009**, *65*, 148–155. [[CrossRef](#)]
64. Turner, M.J.; McKinnon, J.J.; Wolff, S.K.; Grimwood, D.J.; Spackman, P.R.; Jayatilaka, D.; Spackman, M.A. *Crystal Explorer 17*; University of Western Australia: Perth, Australia, 2017. Available online: <http://hirshfeldsurface.net> (accessed on 12 June 2017).
65. Spackman, M.A.; Jayatilaka, D. Hirshfeld surface analysis. *Cryst. Eng. Comm.* **2009**, *11*, 19–32. [[CrossRef](#)]
66. Spackman, M.A.; McKinnon, J.J. Fingerprinting intermolecular interactions in molecular crystals. *Cryst. Eng. Commun.* **2002**, *4*, 378–392. [[CrossRef](#)]
67. Bernstein, J.; Davis, R.E.; Shimon, L.; Chang, N.-L. Patterns in hydrogen bonding: Functionality and graph set analysis in crystals. *Angew. Chem. Int. Ed. Engl.* **1995**, *34*, 1555–1573. [[CrossRef](#)]
68. McKinnon, J.J.; Jayatilaka, D.; Spackman, M.A. Towards quantitative analysis of intermolecular interactions with Hirshfeld surfaces. *Chem. Commun.* **2007**, *37*, 3814–3816. [[CrossRef](#)] [[PubMed](#)]
69. Ok, K.M.; Halasyamani, P.S.; Casanova, D.; Llunell, M.; Alvarez, S. Distortions in Octahedrally Coordinated  $d^0$  Transition Metal Oxides: A Continuous Symmetry Measures Approach. *Chem. Mater.* **2006**, *18*, 3176–3183. [[CrossRef](#)]
70. Santiago, A.; David, A.; Llunell, M.; Pinsky, M. Continuous symmetry maps and shape classification. The case of six-coordinated metal compounds. *New J. Chem.* **2002**, *26*, 996–1009.
71. Hagit, Z.; Shmuel, P.; David, A. Continuous symmetry measures. *J. Am. Chem. Soc.* **1992**, *114*, 7843–7851.
72. Keinan, S.; Avnir, D. Quantitative Symmetry in Structure–Activity Correlations: The Near  $C_2$  Symmetry of Inhibitor/HIV Protease Complexes. *J. Am. Chem. Soc.* **2000**, *122*, 4378–4384. [[CrossRef](#)]